

Review Responses and Revision Changes for Manuscript: Basal control of supraglacial meltwater catchments on the Greenland Ice Sheet

Josh Crozier, Leif Karlstrom, and Kang Yang

We would like to thank both referees for their constructive comments on our submission. We here present point-by-point responses to their comments, and outline the changes we have made in our manuscript accordingly. We expect that these changes have produced a greatly improved manuscript that informs bed-to-surface connections on the Greenland Ice Sheet, and supraglacial hydrology generally. We have attempted to better highlight the contributions of our study (see revised conclusions section).

Key changes in our manuscript include restructuring to better contextualize the geomorphology/meltwater routing parts of our analysis, more thoroughly explaining our model, data, and parameter choices (including addressing seasonality, bed DEM limitations, and slip ratio values), more clearly highlighting our results, and making our figures and discussions more concise.

We note that in our responses all references to specific manuscript sections or figures refer to the revised manuscript unless otherwise indicated, but that text in the Referee comments is unaltered and thus references our original submission .

Responses to Referee #1:

This paper uses previously established transfer functions to make three points:

1) that 1-10 km scale topography on the ice sheet is controlled by bed topography. I don't disagree with this statement because its more or less the conventional wisdom and others have demonstrated this to be the case. It is certainly not new and I don't feel the results presented really shed any new insight relative to Greenland.

Response: That bed topography controls or strongly influences ice surface topography has been mentioned previously in literature. We have cited many of the authors that discuss this link. However, we disagree that our work is not useful in the context of Greenland. We are not aware of any publications explicitly and quantitatively testing this idea using 2D bedrock DEMs, or of any publications quantitatively examining how well bed topography explains 2D ice sheet surface topography as a function of wavelength. Our approach is useful in that we have demonstrated that a relatively simple and easy-to-implement analytical model can explain most IDC-scale (1-10 km) surface topography.

2) Changes in sliding will radically alter the surface topography and catchments, leading to smaller catchments with more moulins and less efficient drainage. This point is somewhat of a stretch given that the high sliding really only occurs in the summer – most of the evolution of the glacier takes place over the other 9 or 10 months of the year.

Response: The hypothesis that changes in surface drainage basins could affect subglacial drainage efficiency which would then affect long-term averaged basal sliding is supported by the sensitivity of bed transfer functions to changes in basal sliding. Testing this hypothesis would be an interesting direction for future work. The seasonal dynamics of ice sheets are of course incredibly important, which we acknowledge in sections 2.1 and 2.3.2, but we do not attempt to model such short time scales in this

work. Seasonal dynamics may be part of the reason why the ice surface topography we predict with transfer functions often exhibits not insignificant deviation from surface DEMs.

However, the transfer functions indicate that the wavelengths of features we focus on should change over timescales of 3-60 years, with minimal seasonal variation (see section 2.3.2). We also point out (consistent with the referee's later statement) that we are not aware of observations indicating that IDC-Scale ice surface topography generally changes significantly on a seasonal basis. If the ice surface topography doesn't change significantly on a seasonal basis but other ice flow parameters do vary, then it is reasonable to question how the "long-term effective (or average)" ice flow parameters that govern surface topography relate to the dynamic ice flow parameters (i.e., annual average or peak values). We do not attempt to address this in our work.

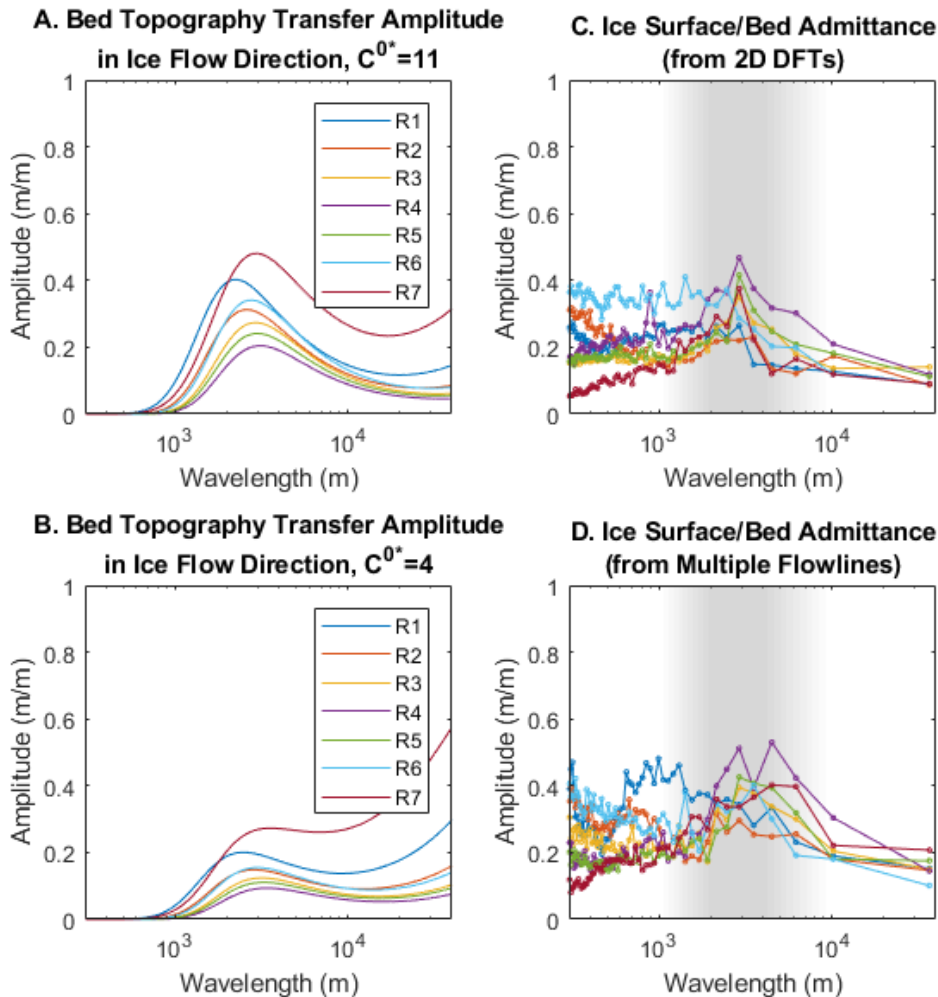
Moreover, they appear to use a very high slip ratio of 11 given that from what I can tell its derived using winter velocities in regions with quite warm (perhaps even temperate ice), with high slopes, so one would expect deformation to be significant (~50/50 as Ryser et al, JGlac 2014 show). Ryser et al show slip ratios this high in summer, but only for a few brief peaks each summer (the annual average slip ratio is much lower). Citing this work as well as others on actual slip ratios would make sense. From Figure 6, its seems like the misfit is somewhat insensitive (broad minimum) to this parameter, so how is the ice sheet so sensitive to change in sliding. In short, the feedback they suggest between catchment size and sliding is not at all well supported. It's also not clear how much faith we should put in a theory derived for small perturbations applied to high-amplitude topography with a linear rheology in place of a non-linear rheology. Such cases can be illustrative, but one has to be careful about then inverting and assigning too much quantitative credence to the results.

Response: A slip ratio of 11 is indeed at the high end of the ranges presented for our study regions in other publications (such as the suggested Ryser et al 2014 which we have referenced in our revision, or our original reference MacGregor et al 2016), even for summer values. We chose a slip ratio of 11 based on the best fitting values found from inversions in study regions with reliable inversion results. However, the inversion minima is often broad (as indicated by figure 5), and so in some regions we could choose a slip ratio as small as around 4 without obtaining significantly worse surface predictions. We expect that the high values of slip ratio we found primarily reflect the assumption of Newtonian ice rheology that is used in the transfer functions. The analysis of Raymond and Gudmundsson (2005) shows that non-linear rheologies generally increase transfer amplitude peak for a given sliding value, thus linear rheology will predict larger basal slip ratios to attain a given transfer peak amplitude (see section 2.3.3). Raymond and Gudmundsson (2005) also demonstrate that the shape of the transfer function as a function of wavelength is generally quite similar between Newtonian and power law ice rheologies.

Using smaller values for slip ratio would not greatly impact some of our primary conclusions so long as the slip ratios used are not smaller than around 2-4. For the amplitude spectra comparisons we cover in sections 2.3.5, 3.1, and figure 7, using a smaller slip ratio does not strongly change the general shape of the transfer function or location of the transfer amplitude peak. This is implied by figure 3, and we have included a modified version of figure 7 in this response (Response Figure 1) to show that for ice flow parameters representative of our region of interest we still predict similar 1-10 km transfer peaks with a slip ratio of 4. Since the wavelengths of peak bed transfer are relatively insensitive to sliding, our conclusion that bed topography transfer can explain the conformity metrics would still be valid (section 3.2.2 and figure 10). Additionally, the slope of our calculated slope-area trends on synthetic flow

networks (figure 9) might decrease if we predict surfaces using lower slip ratios, though the point that bed topography transfer alone can create negative slope-area relations like those observed in stream networks will still be valid (section 3.2.1). Our discussion that focuses in relative changes to basal sliding will also be robust for different baseline sliding choices. As we show in section 4.1 and figure 11, changing slip ratio alters surface topographic basin configuration. This is not inherently inconsistent with the broad constraints that our inversions place on slip ratio, which reflects both bedrock DEM errors and simplifying model assumptions. By showing that different regions of the GIS with a range of ice flow parameters can be reasonably well modeled given sufficiently accurate bed DEMs, we can extrapolate to predict approximate changes in surface topography (and basal hydraulic potential) upon varying ice flow parameters. In other words, we quantify how well the transfer functions work and their sensitivity to bed DEM error, show that they can produce surface topography with sufficient accuracy as to be useful for making general predictions, and then use them as a means to quantitatively predict changes in surface meltwater routing.

Changes: In our revision we have used a slip ratio of 10 instead of 11, since 10 is typically considered a more “round” number, and may better imply that we have just picked an approximate value that produces reasonable results in our study regions with the transfer functions we use. We have also attempted to distinctly refer to the “long-term averaged basal sliding parameter” we use in the transfer functions, so as to not imply we expect this parameter is exactly equal to “slip ratio”. We have also presented more slip ratio inversion results (table 1). We added discussion of the points listed above in section 2.3.3.



Response Figure 1. Demonstration that lower values of slip ratio (C^{0*}) still predict bed topography transfer peaks at wavelengths from 1-10 km (panel B), but less effectively match observed admittances. This figure is similar to figure 10 in our revision except for the additional panel B.

3) There is a lot about thermal-erosion that's not really well explained. There numerous cases where major drainages are observed to be bridged due to large melt channels. So, I am not really sure what the major point is.

Response: We are not claiming that large-scale surface topographic features fully control stream network and drainage basin structure, and the possibility that fluvial processes contribute to internally drained basin reorganization on a seasonal scale is not ruled out by our work. Rather, we find that, in all the regions we examined, the general network-wide structure of supraglacial stream networks and the approximate configuration and number density of IDCs can be explained by bedrock transfer. We did not attempt to carry our more rigorous statistical studies over larger regions; this will become more tractable as bed DEM data improves. The fact that we can predict the large-scale basin structure reasonably well from only bed topography, even using a fairly simple ice flow model, verifies that basal processes are the first-order control on IDC-scale surface topography and meltwater routing, a point that has important implications which we explore in our discussion.

Changes: We removed extraneous discussions of thermal-erosion, and restructured the rest to better illustrate the relation to bed topography transfer and to our key points. For example, we shifted many points from discussion section 4.3 to section 2.4.1 to better introduce the ideas behind the geomorphological metrics we use.

Nearly every Figure is referenced parenthetically, without ever explaining what the figure is supposed to be showing. Statements like “We computed xyz results to make some point. The results show that. . .” Would be helpful. The captions themselves are generally terse and don’t really explain the figures well, especially without supporting explanation in the text. In some cases, the figures appear to be referred to out of order (5 before 4). With respect to the number of figures, this is probably a case of less is more (i.e., fewer, better explained, and more relevant figures).

Changes: We better contextualized figure references and added more explanation to the captions. We removed the old figure 2. We simplified figure 4 but left it in place as we believe it provides a useful and concise illustration of the transfer functions that underlie much of our work for unfamiliar readers, and it also shows that for the parameters we are interested in basal sliding variations have a comparatively minimal effect on surface topography. We moved the old figure 4 to a supplement. We modified figure 6 to better illustrate the stream conformity metrics, and removed the tangential stream elevation profile plot. We simplified the transfer results example figure (figure 8). We made the slope-area figure (figure 9) more clear and comprehensive. Lastly, we removed synthetic flow network results from the conformity metrics figure (figure 10) since these did not contribute to the intended point.

The appendix seems to be largely a rehash of Gudmundson’s work with a few symbols changed. A whole section to define Fourier transforms is unwarranted.

Changes: We removed these appendices.

In summary, I don’t see that this paper adds much new knowledge or insight in its present form. It probably needs a complete restructuring and rewrite.

Response: We agree that restructuring has make our points more clear and better supported them. Though there is of course much room for future work on the ideas we examine, we do believe that our work makes three primary and worthwhile contributions, as stated in the conclusions (section 5) of our revision.

Specific Points

P1/L18 – disperse -> dispersed P1/L18/19 – more dispersed yes, but under the scenarios that would reach this point, the volume of melt water would be greater (i.e., warming world), so it is not clear whether the efficiency would increase or decrease.

Response: A good point. While an examination of potential subglacial-supraglacial feedbacks is a natural extension of our work, there are basic aspects of subglacial hydrology that are still poorly known.

Changes:We added this to section 4.2 of our discussion. We made clearer in this section that our approach simply indicates that there is plausibly some feedback between surface topography, surface hydrology, and basal hydrology.

P2/L18 – set however off with commas (, however,)

P2 L26/27 – would be appropriate to cite Joughin et al 2013 Cryosphere here (and perhaps elsewhere). Their paper has a quite a bit of discussion on the interaction of basal and surface topography and the effect of water routing.

Changes: Implemented both of the above suggestions.

P2 L31 – insert a comma before “which” P3 L6 – “it is unclear whether dynamic stream incision is efficient enough compared to other topographic influences to influence IDC scale topography and meltwater routing” Not sure I understand this statement – as noted below, a quick google search can turn up many pictures see large stream channels cut by overtopping streams.

Response: It has not yet been demonstrated how significant of a role thermal-fluvial incision plays in setting the large-scale structure and evolution of subglacial drainage basins, relative to how much of this structure is primarily set by bed topography. Certainly there are local examples of fluvial erosion influencing drainage patterns, but we show that the effect of bed topography filtered through to the surface appears to be the primary influence on larger scales (longer wavelengths), and is generally of larger amplitude than the effect seasonally averaged fluvial incision has at carving out topography on these scales.

P3 L24 – don’t make Greenland Ice Sheet an acronym as GIS is too commonly used for mapping. You are not word constrained and in most cases you can be brief by just saying Greenland or the ice sheet. P2 paragraph that starts with L20 or L26 – there probably should be a reference to Smith, Raymond, and Scambos 2006, JGR F101019 as they look at the transfer of bed topography to the surface of the Greenland ice sheet. Their findings with respect to anisotropy would make sense to discuss later in the paper as well. P3 L31 – replace “resolution” with “posting” as you note in the next couple of sentences the resolution is anything but 150 m. Ditto for P4 L 2, and L3 (using sampling spacing if you want to avoid repetitive use of posting). P4 L4 – “All” to “The” P4 L14 – Define RSF. P5 16 – hyphenate no-flow condition P13 L26 add a “the” before “~1-10” P13 L30 This is almost identically restates what was said 4 lines earlier. P14 L1-1 again somewhat repetitive and somewhat repeating the obvious that could be inferred from previous work with transfer functions and observations of bed and surface topography.

Changes: Made changes according to the above suggestions.

P14 L16-17 – “If ice surface adjustments to variable basal conditions or ice flow perturbations are sufficiently rapid, surface topographic basin configuration should also vary on seasonal timescales.” If this were the case, then such changes should be occurring now. To the extent any such changes have occurred they escaped notice of numerous groups observing elevation time series.

Response: We are not aware of any studies that have explicitly examined this (point GPS measurements are not ideal for basin-scale deformation), but if there are generally no significant changes in supraglacial topographic basin configuration then our long-term averaged surface predictions could be considered more robust, since there would be a lower potential for inaccuracy due to seasonal dynamics.

Changes: We changed the statement to point out that minimal seasonal adjustment of surface topography is predicted according to the transfer functions.

L14 L24-25 “basal sliding” its important to keep in mind the periods of strong basal sliding relatively brief and most of the year there is no surface melt, so this period of low sliding likely dominates the transfer of bed to surface topography. This statement also applies to the following paragraph. P15-L5-10 – again the winter pattern is likely to dominate and offsets any summer change with a wholesale redistribution of the drainage patterns.

Response: We cannot say from our current methods/data if just winter slip ratio influences topography, or if seasonal speedups matter. However, it does not seem unreasonable to propose that summer sliding rates might have some impact on the long-term averaged ice sheet surface topography, unless the ice surface fully readjusts to changing flow each season (which as previously discussed seems unlikely). We additionally note that long-term changes in atmospheric temperatures could change the length of time each year over which increased sliding occurs, whether or not sliding rates are affected.

Changes: We clarified in both locations that we are referring to changes to “long term averaged basal sliding”.

P15 Section 4.3 There is a significant amount of thermal-fluvial erosion – most stream channels are down-cut by by 10s of centimeters to meters. There are many examples of large stream channels – simple google meltwater stream channels Greenland and select the images tab. The really deep ones are not necessarily that common, but they often occur in locations where a major drainage catchment feeds a lake, that overtops, cut a channel many meters deep, to connect up with another drainage or to find a moulin. I think part of the problem with this section is that its poorly written and its not really clear the point the authors are trying to make.

Response: We have indeed published on the potential influence of fluvial erosion on Greenland ice sheet topography (Karlstrom et al., JGR, 2013, Karlstrom and Yang, GRL, 2016). This influence is undeniable on small scales. But bed topography filtered through to the surface is of larger amplitude than seasonal fluvial-incision in most places, so basin-scale structures are essentially static year to year - this may also be seen clearly on Google Earth (also see Fig 1 of Karlstrom and Yang 2016). We are focusing on what primarily controls basin-scale meltwater routing here, and restructured the text to make this more clear.

Responses to Referee #2:

Summary

This paper explores the factors controlling the catchments of surface rivers on the western Greenland Ice Sheet. It focuses on the relationship between basal topography and these rivers, and concludes that certain geometric aspects (basal bumps and the basal slip ratio) control the organization of surface hydrology. From there, a possible ice-flow feedback is hypothesized based on future projected changes in melt rate and slip ratio. The sign of the ice-flow feedback is unknown.

The study emphasizes the methods (Laplace-domain transfer functions) and most of the results presented (transfer function amplitudes) are a step away from reality, limiting the extent to which results are compared to data. Accordingly, the Results section is very brief (2 pages) compared to the rest of the manuscript (17 pages + Appendix) and the Methods section (8 pages). Phrases like "as expected" or "consistent with previous work" appear frequently, highlighting that this study is light on novel contributions. Most of the 3-page Discussion is speculative and only loosely constrained by the results presented.

Response: We attempted to use the best data-sets available, but given that there were still limitations in data quality for important factors such as bed elevation, we chose modeling approaches (basal transfer functions and surface flow routing) that are simple to interpret, apply, and generalize despite limitations in accuracy. Our evaluation and presentation metrics (amplitude spectra, slope-vs-drainage area trends, and stream network conformity values) capture general traits of surface topography and stream networks that are robust in data and should not depend greatly on our model simplifications. These metrics form the basis for a quantitative verification, using new datasets over multiple regions of the Greenland Ice Sheet ablation zone, of the extent to which bed topography explains surface topography and meltwater routing. Such a verification sets the stage for future more fully mechanistic studies. Our approach also permits the (testable) prediction of surface topography and drainage basin configurations in different ice flow conditions. These predictions indicate that changing ice flow conditions can appreciably affect supraglacial IDC configurations, which is a novel and significant point that we hope will spark further study.

Changes: Our revision includes a more thorough presentation of results and a restructured discussion with explicit calculations of subglacial hydraulic flow pathways and supraglacial IDC configurations (sections 4.1 and 4.2).

The study design is flawed in that the root data (Morlighem bed DEM) are not independent of the validation data (ArcticDEM for the ice-sheet surface) in the regions the authors chose to study (which are, incidentally, areas where Morlighem applied mass conservation). The authors also studied one area (R7) where mass conservation was not applied; results there are not shown, but I would expect their predicted surface to more poorly match the true (Arctic DEM) surface. This is hinted at in Figure 9, but never addressed. The techniques used to generate the bed DEM must be considered in this analysis; preferably, multiple regions with bed DEM constructed from mass conservation and with kriging should be analyzed and compared to one another.

Response: The primary regions we examine are areas where mass conservation (based on surface elevation, velocity, and surface+bed mass balances) is used in conjunction with radar data to derive BedMachine DEMs. As discussed in section 2.2, we are interested in regions that exhibit significant supraglacial stream network development (typically at moderate elevations), near-uniform surface velocities, and that have high resolution surface DEMs. Such regions of the ice sheet seem to generally be where mass conservation instead of kriging was used. However, we expect that BedMachine is the best choice for our study due to three reasons:

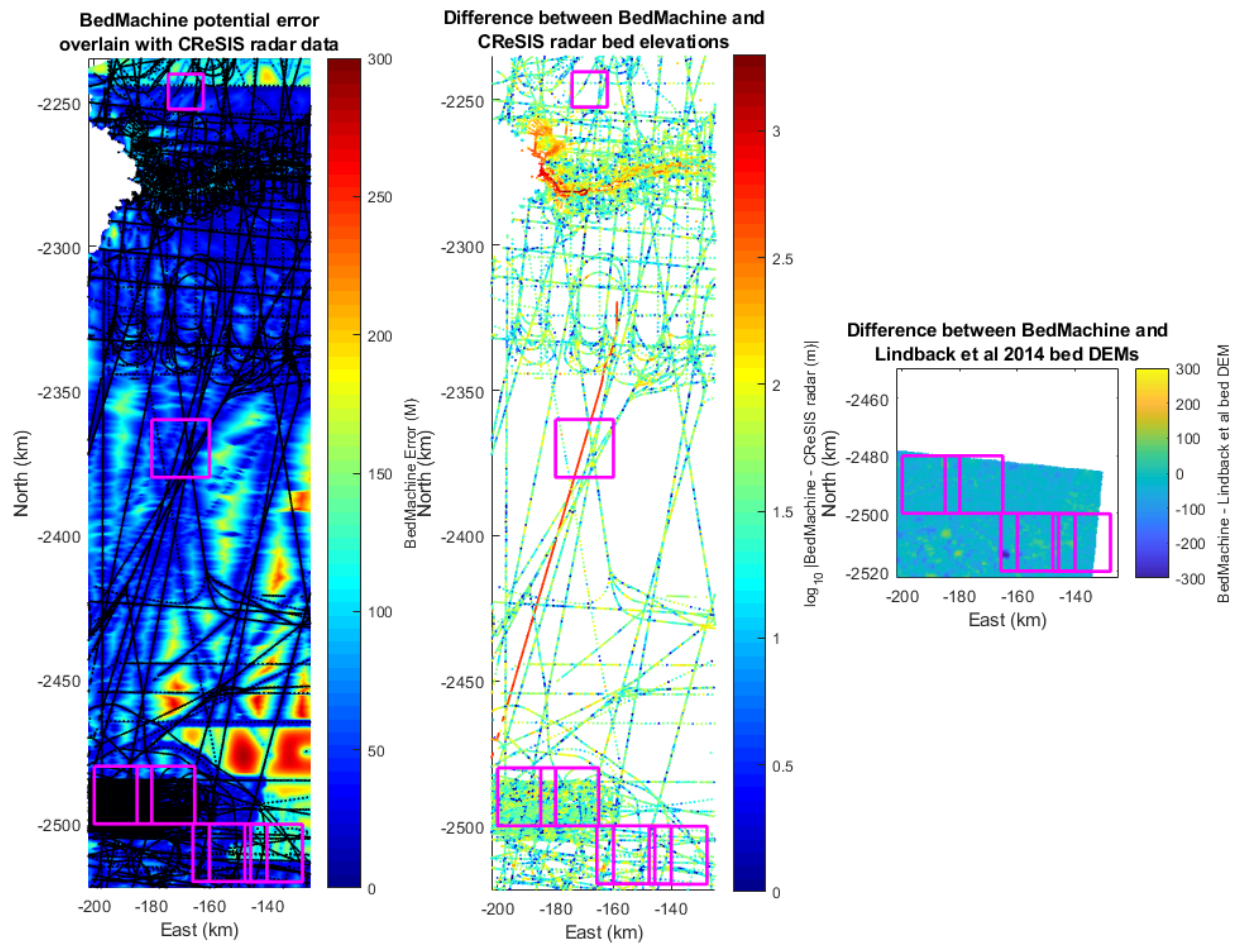
- (1) As far as we are aware, BedMachine is the most accurate Greenland bed DEM currently available, due in part to its use of mass conservation modeling which has advantages described in Morlighem et al (2011) and Morlighem et al (2014).
- (2) The method used in derivation of the BedMachine DEM only considers mass conservation, and is thus fundamentally different from the Gudmundsson transfer functions which are derived from both mass conservation and the Stokes flow equations.

We provide a thought experiment to demonstrate this distinction: given a bed elevation DEM, we could apply the BedMachine mass conservation method in reverse to predict steady-state surface elevations. Doing this uniquely would require a full surface velocity map, in addition to target values of background thickness and surface slope (and basal/surface mass balances if those are not assumed to be zero). The transfer functions make surface elevation predictions given the same target thickness and slope values, but just a single background surface velocity vector and a value/values for slip ratio. The transfer functions are thus also independently solving for a full velocity field by incorporating approximations of how ice should flow in response to gravity and pressure gradients. If we fed the same data we use to implement the transfer functions into an “inverse BedMachine model”, by using single velocity vector and uniform mass balances over the whole domain, the methods would in general not predict the same surfaces.

By verifying that the transfer functions can reasonably well predict the ice surfaces in our study regions, what we are verifying is that the approximations used to derive of the transfer functions are reasonably effective at least over 1-10 km scales. Furthermore, since where mass conservation modeling was used in the BedMachine DEM the mass balance terms were not perturbed to account for spatially nonuniform processes like fluvial incision, we are verifying that most of the ice surface topography at these scales is consistent with ice flow alone.

- (3) We included regions with relatively dense radar coverage, so the influence on mass conservation derived DEMs of surface data will be limited. The analysis we use for testing the possible effect of bed DEM error on our surface predictions, covered in section 2.3.4, 3.1 (see figures 2 and 8.D) provides an indirect indicator of how sensitive our surface predictions are to the mass conservation modeling used in the BedMachine DEMs. This is the case because the published BedMachine error generally increases with increasing distance from radar data points. See the included response figure 2 for further elaboration on this. Our error analysis thus essentially demonstrates that in regions of dense radar coverage, the large-scale surface depressions/ridges we focus on should not be too significantly influenced by the topography between radar transects, and thus by the extrapolation method is used.

We could attempt to obtain raw radar data for our study areas and interpolate it into DEMs using a method like kriging, but this would mean using less accurate bed elevation values (Morlighem et al 2014), and it is not clear that doing so would significantly impact our results or interpretations.



Response Figure 2. Left panel: Error in the BedMachine v3 bed DEM generally increases with increasing distance from radar data (all bed picks from CReSIS shown in black), and our study regions (magenta boxes) are in areas where error is mostly less than around 100 m.

Center panel: Bedmachine elevations are generally in agreement with CReSIS radar data (radar data is colored by interpolated distance from BedMachine values). Some of the deviation of radar elevation points from BedMachine values may be due to error in the radar picks. Radar picks separated by hundreds of meters or less often exhibit hundreds of meters in elevation difference, meaning that a DEM perfectly conforming to radar data would frequently exhibit extremely (likely artificially) high relief.

Right panel: Lindback et al (2014) produced a Greenland bed DEM without mass conservation modeling. In places this differs appreciably from BedMachine, but where the DEM overlaps with our study regions they mostly do not differ too significantly (generally < 100 m). We note that BedMachine v3 incorporates more recent radar data than was available for the Lindback et al DEM.

Overall, this figure demonstrates that the BedMachine DEM agrees reasonably well with radar data, and that using an alternatively derived DEM would not necessarily benefit our study. We added a similar figure to our revision (figure 2).

Changes: We have added a condensed version of the discussion above to section 2.2. We have also added a simplified version of response figure 2 (figure 2), and added the mean bed DEM error in each region to table 1.

The primary question of the study (see first sentence of this review) is interesting and potentially compelling over the next hundred years or so. However, the methods address it incompletely (surface processes, such as fluvial erosion, are only speculated on) and suffer from a considerable flaw in using a bed DEM informed by the surface topography. The paper is out of balance and difficult to follow. If the authors can restructure the manuscript, address the data issues, and either refocus the central question on basal control alone or add treatment of surface-based topographic controls, this would become a worthy contribution.

Response: We hope that our revision and response to this review have addressed questions of data and methodology. We believe that our revised manuscript does more clearly answer the question in the first sentence of this review, at least over the IDC-scales we focus on. Namely, we use multiple geomorphological metrics in combination with a simple method for predicting surface topography over an underlying bed to demonstrate that bed topography can generally explain surface catchment structure at IDC-scales, and that fluvial incision is thus a secondary and generally comparatively minimal influence at such scales. Using a more complex model for surface processes (such as fluvial incision) coupled with ice flow would be a natural and potentially interesting extension of our work, but we expect the results and ideas we present here are still novel contributions and are useful in part because of their generality.

Specific comments

The best-fit value of $C_0^ = 11$ reported here is, as pointed out by Reviewer 1, anomalously high compared to field observations. This is especially important because the authors identify C_0^* as a parameter that IDC density is most sensitive to (Figure 12); thus, it would seem crucial to use a realistic value of C_0^* . The authors' finding of $C_0^* = 11$ by their techniques thus suggests either (1) that other techniques should be used to find a more realistic C_0^* before this analysis is continued, or (2) if the authors are confident in $C_0^* = 11$, the meaning and implications should be explored, which could be an interesting result.*

Response: Refer to our earlier response to Referee 1.

A good paper can demonstrate much of its message through its figures alone. In this case, it is hard to follow the meaning of the figures, which are too many in number (12) and too focused on the methods, which are already well established (Gudmundsson 2003 and other work since). However, this can be readily improved. Recommendations for the figures:

Figure 1: Adapt but keep. Zoom in better on Panel A. Add labels to Panel B – is this the ArcticDEM surface, or a predicted surface?

Changes: Implemented suggestions.

Figure 2: Unnecessary and repetitive from earlier work, remove. Phase is not a big part of the analysis, consider discarding or at least deemphasizing (no figures on phase).

Changes: Removed.

Figure 3: Could adapt and keep. Is panel B correct: thin ice ($H=500$ m) will best express bedrock features of 100 km scale?

Response: For all sets of ice flow parameters (excluding some values as zeros/infinities) as wavelength increases predicted transfer amplitude eventually approaches 1. However, we note that the transfer functions are not valid out to arbitrarily long wavelengths; at length scales very large compared to ice thickness the background gravity current profile of flowing ice will dominate. We also note that the figure is designed to highlight the effect of changing individual ice flow parameters, but that in reality the parameters are not independent.

Figure 4: Unnecessary; remove.

Response: We note that another group has a paper recently accepted for publication (Ignezi et al 2018) using the transfer functions only along flowlines, and thus feel that this figure is relevant in that it illustrates the importance of dimensionality in implementing the linear transfer functions.

Changes: We moved this figure (and some of the corresponding text from section 2.3.2) to a supplement.

Figure 5: Unnecessary; remove all except Panel E, which could be incorporated into Figure 3.

Changes: We removed unnecessary panels from this figure, but kept part of it in the revision as we expect it will provide both a useful visualization of the transfer functions for unfamiliar readers, and an illustration of transfer properties in the specific ice flow regime we examine in this study.

Figure 6: Potentially useful, but why is the misfit pattern so sensitive to η ? How many values of η were tested, and why is the misfit so concentrated at 1015 Pa s? Not what I would expect.

Response: We explored values of effective Newtonian viscosity η ranging from 10^1 to 10^{20} . Holding other ice flow parameters fixed to reasonable values for our study regions, decreasing η generally shifts the transfer function peak to shorter wavelengths. Because our domain sizes (and maximum resolvable wavelengths) are limited, at values of η above around 10^{16} the transfer peak is shifted to high enough wavelengths that there is essentially no transfer calculated. At viscosities around 10^{15} the transfer peak occurs near the longest wavelengths we resolve (around 50-100 km), which does a very poor job of predicting the ice surface. The misfit is particularly large in this part of the parameter space because bed topography amplitude generally increases with wavelength, so a strong expression of these large features creates very unrealistic surface predictions. The changing of the transfer functions becomes much more gradual as effective viscosity decreases beyond around 10^{13} , which is why there is minimal change in misfit at low values of η .

Figure 7: Keep; make color scales the same on Panels E and F.

Changes: We removed the left panels from this figure since this information appears in other figures in some form. Color scales in Panels E and F (C and D in the revision) should cover different value ranges, we used a different color scheme for panel C so as to avoid confusion.

Figure 8: Panel B is not useful. Are the data shown in Panel A from this paper, or previous work? Consider deleting entirely.

Response: Panel A is from our analysis of published data (Karlstrom 2016).

Changes: We replaced panel B with an illustration of the conformity metrics, which we expect will be helpful based upon feedback in these reviews. We moved the stream profiles plot, which is not directly part of our results but which motivates thoughts about the processes shaping stream profiles, to a supplement.

Figure 9: Panel A is misleading because the Stream Free Region (RSF) looks different from all other regions, which may be intended to show the influence of streams. Yet the cause is simply much different H , u , and α in this region compared to other regions (Table 1). For better fidelity, the authors should select a RSF with similar ice geometry to the stream regions.

Response: This figure was not meant to demonstrate anything about streams, but the point that RSF is too different from our other regions to make such demonstrations is valid.

Changes: Since it may prove impossible to find replacement regions with ideal attributes and data availability, and since the stream-free region does not contribute significantly to our analysis anyways, we removed this study region from all analysis in our revision.

Figure 10: Even after a lot of thought, I am still not sure what is being plotted here. I understand the meanings of $\%d$ and Δ , but cannot understand the choice on the y-axis (difference from maximum). In the text, a normalized framework (0 to 1) is discussed, but the data here are not shown that way. The text also highlights variability at small wavelengths (P13 L6-11), but the figure presentation makes this information uninterpretable (all curves are plotted too densely at low wavelengths). Regardless, I infer that the point of this figure is to show the natural variability in both $\%d$ and Δ , by showing the values across R1-R7, and then comparing to the flow networks. For Δ , the flow networks fall within the natural variability, but for $\%d$, it does not. This could suggest something about the control of fluvial erosion, or other surface processes, on surface topography, but this is not addressed.

Response: This figure demonstrates that topographic wavelengths between 1-10 km are important and sufficient for explaining observed stream network structure (according to these metrics). We better described the conformity metrics and this figure, as well as including an illustration of the conformity metrics in figure 6. We normalized the y-axis to highlight that conformity values in all networks plateau and exhibit minimal change as wavelengths smaller than 1 km are added, without this the plots are very messy and are more difficult to interpret. The natural variability in the conformity metrics between regions is interesting, but we do not attempt to explain such variability in this work.

Changes: We removed the synthetic flow network results since they do not contribute to the main point of the figure (that conformity of synthetic flow networks would change over bed transfer wavelengths is expected, since the networks are made on surfaces derived solely from bed topography transfer).

Figure 11: Panel A is not necessary, but Panel B presents a comparison of inferred surface to actual surface, which is essential. Why were such comparisons not run on all 7 study regions? Yet, the text (P13 L16-20) declares the slope-area metric to be of limited utility, according to previous work and data from this study. Thus, any conclusions based on this data (P13 L21-27, P14 L1-2) should be de-emphasized or removed.

Response: The finding that similar slope-area trends can be produced on surfaces only controlled by bed topography and on fluvially-incised regions of the ice sheet is a key conclusion, since it indicates that if supraglacial fluvial incision has an appreciable impact on stream profiles it is secondary and convolved with the effects of ice flow. This observation supports our hypothesis that bed topography is the dominant control on stream network structure. Furthermore, we expect it is important to present our observations as a caution that negative slope-area trends on ice sheets do not necessarily imply a landscape shaped by fluvial erosion, as is sometimes assumed to be the case in terrestrial landscapes.

Changes: We included synthetic flow network results from all regions (though we mention that we don't expect results from R3, R4, and R5 to be as reliable).

Figure 12: Keep.

I also suggest better distinguishing what is observationally based (e.g., stream networks) from what is computed here using transfer functions (e.g., flow networks).

Changes: We used the term "synthetic flow networks" whenever referring to the flow networks we derive from transfer function predicted surfaces, and "stream networks" or "observed stream networks" elsewhere.

The main conclusion, that "bed topography transfer alone can explain ~1-10 km scale ice sheet surface topography" (P13 L29-30), is not illustrated well in any one figure. It can perhaps be inferred from Figure 7E, but the spatial scale must be eyeballed, rather than shown as the independent variable like in the majority of the figures.

Response: The point is meant to be illustrated in the spatial domain by figure 8.A,B (via the correspondence of surface relief, and qualitative similarity of km-scale topographic features), in the spectral domain by figure 7, and indirectly by the conformity metric plots of figure 10.

Changes: We modified the text and captions to make this more apparent.

The Discussion section is largely uncoupled from the rest of the work. Speculation on changes in basal slipperiness on hourly to seasonal timescales (P14 L28, L33, P15 L1-2) is not relevant to the bed-to-surface propagation this paper addresses, as the stated timescale for adjustment is >3 years (P14 L14). Thus, the hypothesized feedback (increasing melt changes sliding, which changes IDC size, affects local melt water volumes at the bed, which again changes sliding), which operates on seasonal or shorter timescales, is not supported or constrained by the study. It would be an interesting concept if it could be shown, but that is not accomplished here.

Response: We expect that section 4.1 of our discussion is justified by our results, and is a natural extension of our results. Section 4.2 makes testable hypotheses if yearly or multi-year averaged ice flow conditions are considered. We think this discussion is important since it points out potential effects that changing surface topography caused by changing ice flow conditions might have on

subglacial hydrology, in accordance with our predictions from section 4.1. The essential point we meant to make with respect to possible feedbacks is: “If subglacial hydrology affects long-term averaged basal sliding, there could be feedbacks in which subglacial hydrology also effects surface topography and supraglacial hydrology”. We think this possibility is worth mentioning since it seems conceivable that there would be some connection between subglacial hydrology and long-term averaged basal sliding, and if this is the case then the mechanisms we discuss could be important for understanding long-term ice sheet evolution.

Changes: We emphasized that we are considering long-term changes. We have also now included explicit calculations of subglacial water flow pathways in this section. We condensed and clarified discussion of a possible feedback mechanism.

The first paragraph of Section 4.1 reads like the main motivation for the study, and as such should appear in the Introduction.

Changes: We placed versions of these points in the abstract and introduction.

Equations 7 and 8 appear in the Discussion, which is strange, and are not applied to further analysis. They should be removed.

The ideas on fluvial erosion (P16 L1-30) are potentially interesting, but again, are completely unexplored in the work. The statement "Our conformity metric calculations (Fig. 10) are consistent with an external control on supraglacial stream network geometry" (P16 L20-21) is not supported by the work. It may or may not be true, but the data were not shown to demonstrate it.

Response: The statement is consistent with our conformity metric results in that the band of wavelengths important for explaining stream conformity metrics in supraglacial stream networks corresponds well with the wavelengths at which bed topography is predicted to transfer strongly (figure 7).

Changes: We significantly condensed and clarified section 4.3. We placed the explanation of the background ideas behind the slope vs drainage area metric in section 2.4.1, which provides better context as to why we consider this metric in examining how well bed topography can explain supraglacial stream network structure and/or how significant fluvial incision appears to be at shaping such structure. We also better clarified in the results (section 3.3) the primary significance of our findings with respect to the conformity metrics. We reworded “external control” to express the intended meaning “control by bed topography transfer”.

Overall, the base idea is worthy of exploration, but the paper is light on results and heavy on unsupported and speculative discussion, and does not fully consider the limitations of its primary dataset.

Response: We expect that our restructured and more thorough revision better emphasises the findings and implications of our work (as discussed above).

Changes: We condensed and restructured our discussion so that its contents are more direct extensions of our results. We included a condensed form of the argument outlined earlier in the response with

respect to BedMachine (see sections 2.1 and 2.3.4 and figures 2 and 8); we point out that BedMachine is the best product currently available, justify our use of the BedMachine mass conservation derived DEMs, and quantitatively examine the associated error and possible resulting surface prediction variance.

References:

Ryser, C., Lüthi, M., Andrews, L., Hoffman, M., Catania, G., Hawley, R., . . . Kristensen, S. (2014). Sustained high basal motion of the Greenland ice sheet revealed by borehole deformation. *Journal of Glaciology*, 60(222), 647-660. doi:10.3189/2014JoG13J196

MacGregor, J. A., et al. (2016), A synthesis of the basal thermal state of the Greenland Ice Sheet, *J. Geophys. Res. Earth Surf.*, 121, 1328–1350, doi: 10.1002/2015JF003803

Gudmundsson, G. H. (2003), Transmission of basal variability to a glacier surface, *J. Geophys. Res.*, 108, 2253, doi: 10.1029/2002JB002107, B5.

Yang, K., and L. C. Smith (2016), Internally drained catchments dominate supraglacial hydrology of the southwest Greenland Ice Sheet, *J. Geophys. Res. Earth Surf.*, 121, 1891–1910, doi: 10.1002/2016JF003927.

Karlstrom, L. and Yang, K, Fluvial supraglacial landscape evolution on the Greenland Ice Sheet, *Geophysical Research Letters*, 43, 2683–2692, <https://doi.org/10.1002/2016GL067697>, 2016.

Raymond, M. J., and G. H. Gudmundsson (2005), On the relationship between surface and basal properties on glaciers, ice sheets, and ice streams, *J. Geophys. Res.*, 110, B08411, doi:10.1029/2005JB003681.

Ádám Ignéczi, Andrew J. Sole, Stephen J. Livingstone, Felix S. Ng and Kang Yang. (2018). Greenland Ice Sheet surface topography and drainage structure controlled by the transfer of basal variability. *Front. Earth Sci.* doi: 10.3389/feart.2018.00101

Lindbäck, K., Pettersson, R., Doyle, S. H., Helanow, C., Jansson, P., Kristensen, S. S., Stenseng, L., Forsberg, R., and Hubbard, A. L.: High-resolution ice thickness and bed topography of a land-terminating section of the Greenland Ice Sheet, *Earth Syst. Sci. Data*, 6, 331-338, <https://doi.org/10.5194/essd-6-331-2014>, 2014.

Morlighem, M., Rignot, E., Mouginot, J., Seroussi, H., Larour, E. Deeply incised submarine glacial valleys beneath the Greenland ice sheet. *Nature Geoscience*. 2014, 7, 418. <http://dx.doi.org/10.1038/ngeo2167>

Morlighem, M., E. Rignot, H. Seroussi, E. Larour, H. Ben Dhia, and D. Aubry (2011), A mass conservation approach for mapping glacier ice thickness, *Geophys. Res. Lett.*, 38, L19503, doi:10.1029/2011GL048659.

Basal control of supraglacial meltwater catchments on the Greenland Ice Sheet

Josh Crozier¹, Leif Karlstrom¹, and Kang Yang^{2,3}

¹University of Oregon Department of Earth Sciences, Eugene, Oregon, USA

²School of Geography and Ocean Science, Nanjing University, Nanjing 210023, China

³Joint Center for Global Change Studies, Beijing 100875, China

Correspondence: Josh Crozier (crozierjosh1@gmail.com)

Abstract. Ice surface topography controls the ~~primary~~ routing of surface meltwater ~~on~~ generated in the ablation zones of glaciers and ice sheets. Meltwater routing is ~~important for understanding and predicting ice sheet evolution because surface melt can be both~~ a direct source of ice mass loss ~~and an influence on basal sliding and ice advection. Although controls on,~~ as well as a primary influence on subglacial hydrology and basal sliding of the ice sheet. Although the processes that determine ice sheet topography at ~~continental-scales~~ the largest scales are known, controls on the topographic features that influence meltwater routing at ~~drainage basin~~ supraglacial internally-drained-catchment (IDC) scales (< 10s of km) are ~~not well understood less well constrained~~. Here we examine the effects of two processes ~~that can influence on~~ ice sheet surface topography: ~~basal transfer (where ice advection over variable bed topography and basal sliding conditions creates surface expressions), transfer of bed topography to the surface of flowing ice~~ and thermal-fluvial ~~incision (thermal erosion by supraglacial streams)~~ meltwater streams. We implement 2D ~~bed topography and basal sliding~~ basal transfer functions in seven study regions of the western Greenland Ice Sheet ~~(GIS) ablation zone to study the influence of basal conditions on ice surface topography. Although bed elevation data quality is spatially variable, we~~ ablation zone using a suite of recent data sets. We find that ~1-10 km scale ice surface features ~~under variable ice thickness, velocity, and surface slope are well predicted by these transfer functions. We then can be well explained by bed topography transfer in regions with different long-term averaged ice flow conditions. We~~ use flow-routing algorithms to extract supraglacial stream networks from 2-5 m resolution digital elevation models, and compare these with synthetic flow networks calculated on ice surfaces predicted by bed topography transfer. ~~Quantitative comparison of these networks reveals~~ Multiple geomorphological metrics calculated for these networks suggest that bed topography can explain ~~general~~ ~1-10km ~~surface meltwater routing patterns without significant contributions from supraglacial meltwater routing, and that thermal-fluvial erosion by streams. We predict thus has a lesser role in shaping ice surface topography on these scales. We then use bed topography transfer functions and flow-routing to conduct a parameter study predicting~~ how supraglacial internally drained catchment (IDC) ~~patterns on the GIS configurations and subglacial hydraulic potential~~ would change under ~~time-varying varying multi-year averaged~~ ice flow and ~~for~~ basal sliding regimes. ~~Basal sliding variations exert a significant influence~~ Predicted changes to subglacial hydraulic flow pathways directly caused by changing ice surface topography are subtle, but temporal changes in basal sliding or ice thickness have potentially significant influences on IDC spatial distribution, ~~and suggest a potential positive feedback between subglacial hydrologic regime to surface IDC patterning. Increased basal~~

~~sliding will increase IDC spatial density (by decreasing IDC sizes) and cause more disperse meltwater input to the englacial and subglacial environment. This could result in less efficient subglacial channelization and increased basal sliding that would then further increase IDC density.~~ We suggest that changes to IDC size and number density could affect subglacial hydrology primarily by dispersing the englacial/subglacial input of surface meltwater.

5 *Copyright statement.* TEXT

1 Introduction

During ~~warm seasons~~ warmer months on the Greenland ice sheet (GIS) ablation zone, surface melting in the ablation zone generates a large volume of water. Some meltwater is stored in or flows through porous firn (~~compacted snow~~) or weathered ice, but most flows across the ice surface in supraglacial streams (Fountain and Walder, 1998; van den Broeke et al., 2009; Andersen et al., 2015; M
10 ~~forming networks of supraglacial streams and lakes (such as the stream network shown in Fig. 1.B) (Fountain and Walder, 1998; van den B~~

~~.~~ The majority of these streams feed into the ~~subglacial hydrological system~~ englacial and subglacial hydrological systems either by flowing directly through open moulins into open moulins (e.g., Chu, 2014; Smith et al., 2015), or by flowing into supraglacial lakes (e.g., Chu, 2014; Smith et al., 2015; Yang and Smith, 2016; Smith et al., 2017), which can drain when enough water pressure builds up to hydraulically fracture the ice (Das et al., 2008; Selmes et al., 2011; Stevens et al., 2015). Much

15 of the meltwater will ultimately end up in the ocean after flowing through the englacial and subglacial hydrological systems (Enderlin et al., 2014; Andersen et al., 2015). Subglacial water significantly influences (Enderlin et al., 2014; Andersen et al., 2015)

~~.~~ Along the way, subglacial water and temporal variations in subglacial water flux can significantly influence ice advection by reducing/modulating basal sliding resistance, though spatial and temporal water flux are important since the morphology of subglacial hydrologic pathways exerts a strong influence on sliding (e.g., Zwally et al., 2002; Schoof, 2010; Sole et al., 2011; Shannon et al.

20 ~~. Processes associated with the (e.g., Zwally et al., 2002; Schoof, 2010; Sole et al., 2011; Shannon et al., 2013; Tedstone et al., 2014)~~

~~.~~ The spatial and temporal flux of surface meltwater to the subglacial hydrological system, which dictate how this flux evolves with changing climate and/or ice flow, are and how subglacial hydraulic pathways evolve in response to meltwater input, are all poorly constrained and largely not incorporated into current ice sheet mass balance models (Larour et al., 2012; Gillet-Chaulet et al., 2012; Gagliardini et al., 2013; Lipscomb et al., 2013; Khan et al., 2015; Smith et al., 2017).

25 Ice sheet surface meltwater flows downhill as dictated by surface topography. The largest scale of GIS Greenland Ice Sheet topography is a continental-scale (~ 1000 km) gravity current profile, where average surface slope is very gradual in the interior of the ice sheet and steepens approaching the margins (Cuffey and Paterson, 2010). Deviations from this geometry at smaller wavelengths however, however, reflect a combination of other physical processes. Some are products of the surface energy balance, such as solar radiation-driven ice melting/sublimation, melting of ice by flowing surface water (we will refer to this process as thermal-fluvial incision), and snow accumulation (Cuffey and Paterson, 2010; Karlstrom and Yang, 2016; Boisvert et al., 2017; Meyer and Hewitt, 2017). Others are products of ice advection flow processes such as crevassing (Echelmeyer et al.,

1991; Cuffey and Paterson, 2010) ~~and~~, propagating ice flux waves (Weertman, 1958; Nye, 1960; van de Wal and Oerlemans, 1995; Hewitt and Fowler, 2008). ~~Still others involve~~, and the transfer of spatially variable bed topography, basal sliding, and ice rheology (due to temperature, grain alignment, or impurities) to the surface (Gudmundsson, 2003; Raymond and Gudmundsson, 2009; Sergienko, 2013; Graham et al., 2017).

5 The advection of ice over rough bed topography (such as that shown in Fig. 1.A) (~~De Rydt et al., 2013; Yang and Smith, 2016~~) (Budd, 1970; Hutter et al., 1981; Gudmundsson, 2003; De Rydt et al., 2013; Joughin et al., 2013) is thought to be a significant source of IDC scale (~1-10 km) ice surface topography, and is a primary focus of our study. Supraglacial IDC and lake locations generally remain fixed year to year despite ice advection, which suggests a basal controlling process (Lampkin, 2011; Lampkin and van der Berg, 2011; Selmes et al., 2011; Sergienko, 2013; Ádám Ignéczi et al., 2016; Karlstrom and Yang, 2016).

10 We use the term “bed” loosely to refer to whatever material composes the substrate under an ice sheet. In many locations the bed contains a deformable till layer which may not influence ice flow in the same way as rigid bedrock (Tulaczyk et al., 2000; Cuffey and Paterson, 2010), and ~~even rigid~~ bedrock erodes under the action of ice motion (Sugden, 1978; Hart, 1995).

Thermal-fluvial incision is also important for the evolution of surface topography and meltwater channel networks (~~Parker, 1975; Karlstrom~~ ~~Some supraglacial stream channels reform yearly as previous channels are advected by ice flow, though other channels~~ ~~are reused for multiple years (Karlstrom and Yang, 2016). Stream channels (e.g., Parker, 1975). Surface melt rates in many~~ ~~areas of the Greenland Ice Sheet ablation zone are greater than 1 m/yr (Noel et al., 2015); stream channels~~ can be meters deep, and are in places observed to flow in directions not parallel to the surrounding ice surface slope or to slice through topographic ridges ~~altogether~~ (Smith et al., 2015; Yang et al., 2015). Karlstrom and Yang (2016) suggested that longitudinal elevation profiles of supraglacial streams might even be inverted for primary production rate of meltwater, the analog

15 ~~to inferring tectonics-climate variations and tectonic uplift rates~~ from river profiles in terrestrial settings. However, although thermal-fluvial incision is required to make channels in the first place (e.g., lowering rate in channels must be greater than surroundings, ~~Parker, 1975~~), it is unclear whether dynamic stream incision is efficient enough compared to other topographic influences to ~~influence significantly affect~~ IDC-scale topography and meltwater routing. ~~Supraclacial streams in this way In this way supraglacial streams~~ may be more analogous to ephemeral gullies on earth flows (Mackey and Roering, 2011) than

20 ~~to terrestrial river networks. The ice surface in ablation zones advects stream channels horizontally at velocities greater than 100 m/yr (Joughin et al., 2010b, a; Nagler et al., 2015), deforming or offsetting stream networks as they incise. This has been observed where Greenland supraglacial stream channels form along offset but parallel pathways as channels from previous years are advected out of topographic lows during winter months, though there are also stream channels that are reused for multiple years (Karlstrom and Yang, 2016).~~

30 Understanding the relative contributions of processes that govern ablation zone surface topography ~~could yield better means of tracking/predicting the spatial and temporal generation and routing of meltwater. Ice velocity should yield better predictions of meltwater routing through time. Here, we use multiple data sets to examine the effects and significance of bed topography transfer and thermal-fluvial incision on ice sheet surface topography and meltwater routing. Ice surface velocity measurements,~~ high resolution ice surface imagery and ~~elevation models~~ digital elevation models (DEMs), and bed elevation ~~datasets~~ DEMs are now concurrently available over large expanses of the Greenland ice sheet (~~GIS~~) ~~ablation zone~~

35

(ArcticDEM, 2017; Joughin et al., 2010b, a; Helm et al., 2014; Morlighem et al., 2014, 2015; ?; Nagler et al., 2015; Noel et al., 2015) ~~With~~ ablation zone (Joughin et al., 2010b, a; Helm et al., 2014; Morlighem et al., 2017a, b; Nagler et al., 2015; Noel et al., 2015; ArcticDEM). ~~Many of~~ these data sets ~~, we examine the significance and effects of bed topography transfer and thermal-fluvial incision on ice sheet surface topography and meltwater routing,~~ are rapidly increasing in quality and temporal coverage, and developing
5 ~~methods to efficiently integrate such large data sets is thus important.~~

We implement approximate analytical solutions for bed topography transfer through ~~ice (Gudmundsson, 2003) to evaluate the flowing ice (Gudmundsson, 2003) over 2D regions of the Greenland ablation zone, evaluating the~~ extent to which ~~bed topography transfer explains the ice surface in different flow regimes~~this transfer can explain observed ice surface topography as a function of wavelength. To examine ~~what influences~~ supraglacial meltwater routing ~~we apply flow routing,~~ we apply
10 ~~flow-routing~~ algorithms both to ~~the real ice surface~~ ice surface DEMs and to synthetic ice surfaces predicted from modeling bed topography transfer. In the resulting flow networks we examine ~~slope versus channel slope versus accumulated~~ drainage area trends ~~and flow network conformity to various wavelengths of~~ to assess the fluvial erosion signature, and we examine ~~stream network conformity with~~ surrounding ice surface topography ~~to quantify the importance of different wavelengths for explaining stream network spatial structure.~~ We identify bed topography transfer as ~~a~~ the primary control on ~~IDC-scale surface~~
15 ~~topography and~~ meltwater routing, and then use bed topography transfer functions to predict ~~the response of GIS IDCs to changing how Greenland surface IDC configuration and subglacial hydraulic flow pathways would change in response to varying~~ ice flow conditions.

2 Methods

2.1 Data

20 We use stereo imagery derived ~~SETSM~~ ArcticDEM 2-5 m resolution mosaics for 2011 Greenland Ice Sheet (~~GIS~~) surface elevation (ArcticDEM, 2017; Noh and Howat, 2015). These DEMs were created by piecing together smaller DEM strips that in some cases come from data taken over multiple months ~~,~~. ~~This is~~ a potential source of error in our analysis since ice sheet surface topography can vary temporally due to a variety of processes including horizontal ice advection (on the order of 100
25 m/yr ~~, in our study areas~~ (Joughin et al., 2010b, a; Nagler et al., 2015)), ablation (on the order of 1 m/yr (Bartholomew et al., 2011)), accumulation (on the order of 1 m/yr (Koenig et al., 2016)), and advection-related thickening/thinning such as that caused by changes in basal properties (on the order of 1 m/yr (Das et al., 2008; Helm et al., 2014)). ~~We~~ ~~In our study regions~~ ~~we~~ observe $< \sim 1$ m vertical and $< \sim 10$ m horizontal offsets from surface DEM stitching ~~, (where different raw source data sets are combined).~~

We use the Icebridge BedMachine ~~v3~~ 150 m resolution Greenland bed elevation DEM (~~Morlighem et al., 2014, 2015~~), which
30 (~~Morlighem et al., 2017a, b~~). ~~This product~~ is derived from radar ~~and data, and in some regions also from~~ ice mass conservation modeling. This product has ~~very high large~~ error (as much as 500 m) in areas with low radar pass density ~~, which we~~; ~~we~~ ~~selected study regions with a range of bed DEM quality (shown in Fig. 2). Many regions of the ablation zone, including our study regions, are where mass conservation modeling was used to extrapolate raw radar transects into contiguous bedrock~~

DEMs. This approach and its advantages are explained in detail by Morlighem et al. (2011) and Morlighem et al. (2014). Surface elevations, surface velocities, and mass balances estimates are used to produce more accurate Bed DEMs that are consistent with multiple radar-derived data sets which have limited spatial coverage (as shown in Fig. 2). The mass conservation modeling does not preclude us from using these DEMs to evaluate the effectiveness of bed topography transfer functions at predicting surface topography, since the approach used in creating the bed DEMs only solves mass conservation equations and does not take into account ~~when selecting regions for our study, the momentum balance accounted for by the transfer functions~~ (described in Section 2.3.1). However, as an additional precaution, we focus our analysis primarily on regions with more dense radar transect coverage. DEMs in these regions should most closely reflect the raw radar data, and also generally have higher effective resolution.

5 We use 2009 InSAR derived MEASUREs (Joughin et al., 2010b, a) ~~and 2015 optical/SAR derived CCI Sentinel-1 (Nagler et al., 2015)~~ (both data sets are for 500 m resolution) ~~for GIS Greenland winter ice~~ surface velocities. We use Landsat imagery to identify moulins, lakes, and stream channels (Yang and Smith, 2016). We use RACMO 2.3p2 at 1 km resolution for melt data from the full year 2015 (Noel et al., 2015) to indicate relative melting between different regions of ~~the GIS~~ Greenland. All data sets do not necessarily correspond temporally, which is a potential source of error in our analysis since ice velocity, ice surface topography, and bed topography can vary temporally (Sugden, 1978; Hart, 1995; Bartholomew et al., 2011; Sole et al., 2011; Helm et al., 2014). We focus our analysis and discussions on long-term averaged ice flow properties, and do not attempt to model seasonal dynamics.

15

2.2 Study regions

We focus on areas of the ~~GIS ablation zones~~ Greenland Ice Sheet ablation zone that exhibit significant supraglacial drainage networks, ~~that are not heavily crevassed (since dense crevassing can interfere with supraglacial drainage network development), and that, and~~ do not contain ice streams ~~(since ice streams often have very different ice advection and basal sliding properties than pathways where ice is advecting very rapidly relative to the surrounding regions of an ice sheet, and also often have heavily crevassed surfaces)-).~~ We additionally require areas with high resolution (2-5 m) surface DEMs and near-uniform ice surface velocities. Using these criteria we select seven internally drained catchments (IDCs) from the western ~~GIS~~ Greenland Ice Sheet as primary study regions (shown in Fig. 1.A, with additional information in Table ??). These regions cover a significant ~~fraction~~ range of the elevations, ice thicknesses, ice surface slopes, and ice surface velocities over which extensive supraglacial stream networks form (Fig. 1.A). ~~We also examine control region RSF from the eastern GIS that does not exhibit supraglacial streams (Fig. 1.A). For implementing bed topography transfer functions we primarily focus on regions R1 and R2 which exhibit near-uniform surface velocity and accurate bed DEMs, for reasons discussed in sections 2.3.1 and 2.3.2 on western Greenland.~~

20

25

2.3 Bed topography and basal sliding transfer

2.3.1 ~~Transfer function derivation~~ Linear transfer functions

The governing equations of flowing ice are the Stokes equations for conservation of momentum and mass balance for an incompressible fluid. ~~Though ice is better~~ Ice is often described with a nonlinear constitutive relation known as Glen's law (Cuffey and Paterson, 2010), but here a linear Newtonian ice rheology is assumed. Ice rheology is also assumed to be spatially and temporally constant, though the rheology of ice generally varies with temperature, grain geometry, and ~~sediment content~~ impurities. The momentum equations ~~are then given by~~ we solve are

$$\nabla p = \eta \nabla^2 \mathbf{u} + \rho_i \mathbf{g}, \quad (1)$$

where p is pressure, η is effective dynamic ice viscosity, \mathbf{u} is ice velocity, and ρ_i is ice density. Cartesian coordinates are used, where the z -axis is aligned normal to the mean ice surface and the x -axis points in the direction of maximum bed gradient. \mathbf{g} is the gravitational acceleration (in the $-z$ direction). Conservation of mass is given by

$$\nabla \cdot \mathbf{u} = 0. \quad (2)$$

~~We use transfer functions derived by Gudmundsson (2003) to solve~~ Linear stability analysis of Eqs. (1) and (2) ~~and predict by Gudmundsson (2003) provides analytical transfer functions that predict approximate~~ ice surface topography over underlying rough bed topography or basal sliding variations. In the spectral domain, transfer functions are generally of the form ~~$\hat{Y}(\mathbf{k}) = \hat{X}(\mathbf{k})\hat{T}(\mathbf{k})$~~ ~~$\hat{X}_o(\mathbf{k}) = \hat{X}_i(\mathbf{k})\hat{T}(\mathbf{k})$~~ where $\mathbf{k} = (k_x, k_y)$ is a ~~wave-number~~ wavenumber (inverse wavelength) vector, ~~\hat{Y}~~ \hat{X}_o is output data (ice surface elevation in our case), ~~\hat{X}~~ \hat{X}_i is input data (bed elevation in our case), and T is the transfer function relating outputs to inputs. Transfer functions are possible to obtain for linear time-invariant systems; the basic underlying principals are that the output for such systems may be calculated for any single ~~wave-number~~ wavenumber input, that any input may be represented as a sum of individual ~~wave-number~~ wavenumber components via Fourier transform, and that the output will be a sum of the independent outputs from each input component (Stein and Wysession, 2005). In the rest of this section we will ~~briefly describe~~ summarize the derivation of the transfer functions (described fully in ~~(Gudmundsson, 2003)~~ Gudmundsson (2003)) and the important approximations made in this derivation.

Bed ~~erosion is ignored and bed~~ elevation is assumed to not change temporally beyond an initial perturbation. Basal melting/freezing are also ignored, assumptions that are likely reasonable from a mass conservation perspective due to the generally slow rates of basal melting/freezing (Huybrechts, 1996). Basal sliding velocity \mathbf{u}_b is assumed to be governed by a sliding law of the form

$$\mathbf{u}_b(x, y) = C(x, y)\boldsymbol{\tau}_b(x, y) \quad (3)$$

where $\boldsymbol{\tau}_b$ is basal shear stress and C is a sliding parameter. We will often refer to non-dimensionalized basal sliding coefficient $C^* = C \frac{2\eta}{H}$ (approximately equivalent to slip ratio, the ratio of basal sliding velocity to ice deformational velocity). Other forms of sliding law have been proposed (Fowler, 1986; Tulaczyk et al., 2000; Cuffey and Paterson, 2010). The basal boundary

condition (at the bed-surface/bed-ice interface) combines this sliding law with a no-flow/no-flow condition dictating zero ice velocity normal to the boundary. Surface accumulation/ablation are ignored, which is reasonable as both rates are generally small compared to ice advection rates (van den Broeke et al., 2011). The ice surface boundary conditions are zero traction plus the kinematic boundary condition

$$5 \quad \frac{\partial Z}{\partial t} = u_z - u_x \frac{\partial Z}{\partial x} - u_y \frac{\partial Z}{\partial y}. \quad (4)$$

Thus the ice surface boundary is the only source of time variation in the system.

Parameters including ice thickness, surface velocity, and surface slope are assumed to be similar over the domain of interest, which allows for solutions to be obtained as perturbations to a zeroth-order infinite plane slab solution. In order for these assumptions to be valid, it is assumed that bed topography amplitude is much smaller than ice thickness, and that the domain of interest is small compared to the horizontal dimensions of the ice sheet. The zeroth-order ice surface Z^0 is a plane with slope α in the direction of ice flow. Zeroth-order ice thickness H is the mean ice thickness in the domain. Zeroth-order basal shear stress is given by $\tau_b = \rho g H \sin(\alpha)$, and zeroth-order deformational velocity is given by $U_d = \frac{1}{2\eta} \tau_b H$, where ρ is (spatially constant) ice density.

Bed elevation B is expressed as $B = B^0 + \epsilon F_B^\epsilon$, where B^0 is zeroth-order (horizontal plane) bed elevation, F_B^ϵ represents perturbations to B^0 , and $\epsilon =$ bed topography amplitude/ $H \ll 1$. Basal sliding coefficient C is similarly expressed as $C = C^0 + \beta F_C^\beta$ where $0 \leq \beta \ll 1$. Equations 1 and 2 are linearized around $\epsilon, \beta = 0$ and solved in the Fourier domain. Ice surface elevation is then given by

$$Z = Z^0 + \epsilon F_Z^\epsilon + \beta F_Z^\beta + \mathcal{O}(\epsilon^2, \beta^2, \epsilon\beta), \quad (5)$$

where ϵF_Z^ϵ and βF_Z^β represent the first order (linear) ice surface response to B and C perturbations. Higher order terms $\mathcal{O}(\epsilon^2, \beta^2, \epsilon\beta)$ are discarded.

The full time-dependent transfer functions ~~from Gudmundsson (2003) are reproduced in Appendix ??~~ can be found in Gudmundsson (2003). A steady state surface configuration to bed topography and basal sliding perturbations is approached as $t \rightarrow \infty$. We note that ice flow parameters in the transfer functions are not strictly independent, such that there are limited restricted parameter combinations that ~~produce realistic~~ correspond to real ice flow configurations.

~~The~~ Although the linear transfer functions derived by Gudmundsson (2003) (~~Appendix ??~~) do not capture all the complexities of ice motion, ~~as discussed above. However,~~ they have some significant advantages over other methods for solving ice flow problems our desired ice flow problem. They do not make a shallow ice approximation (which ignores longitudinal stresses and thus breaks down at length scales on the order of ice thickness H (e.g., Cuffey and Paterson, 2010)), and are thus valid at spatial scales $< H$. Additionally, they can be efficiently implemented over 2D IDC-scale regions without requiring initial conditions, flow line geometry, and domain-edge boundary conditions that many numerical flow simulators need. ~~Although many of the assumptions made deriving these transfer functions are likely somewhat unrealistic over much of the GIS,~~ We will show that the functions still reproduce general topographic features and amplitude spectra of our Greenland Ice Sheet study regions well, and thus provide a useful predictive tool.

2.3.2 Transfer function implementation

When implementing the transfer functions in all following analysis we will assume the ice surface has reached a steady state in response to the underlying bed topography and basal sliding conditions. To examine the validity this assumption, we calculate the transfer function perturbation adjustment timescales for parameters representative of the western GIS-Greenland ablation zone (from study region R1 (Fig. 1.A, Table ??) with $C^{0*} = 11-10$ and $\eta = 10^{14}$ Pa s) using the time-dependent transfer functions defined in Appendix-??Gudmundsson (2003). For the range of ice flow parameters we are interested in, there is no appreciable downstream advection of surface perturbations(Gudmundsson, 2003), and so the surface response soon after a basal perturbation is essentially a lower amplitude scaling of the steady state (maximum amplitude) surface response. We find that the time scale for bed topography or basal sliding transfer amplitudes to reach 95% of their steady state values is as much as 60 years for the longest wavelengths of topography in our typical study areas (~ 20 km), and is $\sim 3-20$ years for wavelengths that typically exhibit the highest transfer ($\sim 1-10$ km). It is probably unlikely that bed topography, ice sheet thickness, or ice sheet surface slope change significantly over these timescales, but ice velocity and basal sliding can vary on day to year timescales, meaning that the steady state assumption is a potential source of error in our analysis (Das et al., 2008; Bartholomew et al., 2011; Sole et al., 2011; Helm et al., 2014; Chandler et al., 2013)(Das et al., 2008; Bartholomew et al., 2011; Sole et al., 2011; Helm et al., 2014; Chandler et al., 2013)

Methods have recently been developed and applied for implementing the linear basal transfer functions along flowlines with spatially varying parameters (Ignecci et al., 2018; Ng et al., 2018), which allows for implementation of the transfer functions over large regions. However, implementing the transfer functions just along flowlines can result in significant inaccuracy. With ice flow parameters representative of the western Greenland Ice Sheet ablation zone, the transfer amplitude of IDC-scale ($\sim 1-10$ km) bed features predicted by the linear transfer functions could vary by up to a factor of 10 depending upon the 2D alignment of those features (see supplement). Our approach retains the simpler constant-parameter model but accounts for 2D effects. We implement the basal transfer functions over rectangular domains of small enough size (20 km across) that ice flow parameters are relatively uniform within each domain.

To implement the ~~transfer functions, rather than using coordinates aligned in the ice flow direction we use Cartesian~~ coordinates aligned in the transfer functions in (east, north, vertical) ~~directions, thus Cartesian coordinates, we calculate~~ absolute wavenumbers as $k = \|\mathbf{k}\|$ and ($k_U = \frac{\mathbf{k} \cdot \mathbf{U}}{\|\mathbf{U}\|}$ wavenumbers in the ice flow direction as $k_U = \frac{\mathbf{k} \cdot \mathbf{U}}{\|\mathbf{U}\|}$. We can then calculate transfer function matrices (~~$\hat{T}_B(k_x, k_y)$ and $\hat{T}_C(k_x, k_y)$~~) $\hat{T}_B(k_x, k_U)$ and $\hat{T}_C(k_x, k_U)$ corresponding to the discrete wavenumber components of a given bed DEM(Fig. ??).~~Due to the alignment of k_U with the direction of ice flow, the amplitude matrix A is,~~ The amplitude matrices ($|\hat{T}_{B,C}|$) are symmetric about the line perpendicular to this the ice flow direction, and the phase matrix ϕ is matrices ($\arg(\hat{T}_{B,C})$) are anti-symmetric about the line perpendicular this direction this line. The transfer amplitude for bed topographic features aligned with the direction of ice flow approaches one as wavelength approaches infinity, but non-zero values of the basal sliding parameter C^{0*} result in an additional peak in transfer amplitudes at intermediate wavelengths (as illustrated in Fig. 3, Gudmundsson, 2003). Transfer amplitudes approach zero at small wavelengths or as topographic fea-

tures approach a flow-perpendicular alignment (Fig. ??). Transfer function phase shift is also important, and results in a wavelength-dependent offset between bed features and their surface expression (as illustrated in Fig. 4).B).

The two-dimensionality of the transfer functions is important. This can be demonstrated by examining a scenario with different single-wavenumber components of bed topography (plane-waves) that have the same apparent wavenumbers in a transect interpolated across bed topography along an ice flowline (a bed elevation profile along the ice flow direction). The same apparent wavenumber in the ice flow direction k_U could arise from any single wavenumber component of bed topography with absolute wavenumber $k = k_U \cos(\theta)$ aligned at angle θ from the ice flow direction, where the plane-wave ridge alignment is perpendicular to the direction of ice flow when $\theta = 0$. If we evaluate the predicted transfer functions for a given k_U and set $k = k_U \cos(\theta)$ for a range of θ , we can see that the transfer amplitude and phase both depend upon θ , even though the apparent flowline bed topography is the same for all $\theta \neq \frac{n\pi}{2}$ (see equations in Appendix ??). Thus the configuration of bed topography off of a flowline can influence the ice surface over said flowline. With ice flow parameters representative of the western GIS ablation zone, the predicted transfer amplitude of IDC-scale ($\sim 1-10$ km) bed features could vary by up to a factor of 10 depending upon the 2D alignment of those features. (Fig. ??).

Prior to taking 2D discrete Fourier transforms (DFTs, see Perron et al., 2008 for DFT definition for example Press et al., 2007) of bed DEMs, we first shift each bed DEM to have zero mean elevation. We do not detrend bed DEMs, as that is not consistent with the zeroth-order bed conditions. We then mirror each bed DEM in all directions by connecting east-west reversed copies of each DEM to the east and west sides of itself, connecting north-south reversed copies of each DEM to the north and south sides of itself, and connecting north-south and east-west reversed copies of each DEM to all corners of itself. Next we apply a cosine taper such that all elevations along the edges of each mirrored bed DEM are zero, and the original domain in the center is unaffected. These processing steps are taken to minimize edge effects (Perron et al., 2008). We then take 2D DFTs of the mirrored bed DEMs, and use the transfer functions to obtain predicted ice surface elevation Z' as:

$$Z'(x, y) = Z^0(x, y) + \mathcal{F}_D^{-1} \left(\hat{T}_B(k_x, k_y) \hat{B}(k_x, k_y) + \hat{T}_C(k_x, k_y) \hat{C}(k_x, k_y) \right) \quad (6)$$

where B is the zero-mean bed elevation, Z^0 is the zeroth-order ice surface (with average elevation H and slope α , obtained by a plane fit to the actual ice surface elevation ice surface DEM Z), and \mathcal{F}_D^{-1} represents the inverse 2D DFT (see Appendix ??). We then trim enough space from the edges of each predicted surface so that we are only considering a region that will not contain any artificial edge effects.

2.3.3 Ice viscosity and basal sliding estimation

Two important and poorly constrained parameters in our bed topography transfer method are ice viscosity η and basal sliding parameter C^* . One possible application of the transfer functions is to infer/invert for these parameters as a function of space from observed surface and bed DEMs (Raymond and Gudmundsson, 2009). We do not take this approach here. Rather, we are concerned with a more basic assessment of how well ice surface topography can be explained by transfer of basal conditions. However, we do need to choose values for η and C^* .

We ~~first focus on~~ examine the importance of spatial variations in C^* by comparing the predicted ice surface over Gaussian B and C^* perturbations with 2 km standard deviations and 200 m height or 200 C^* amplitude, using ice flow parameters from region R1 (Fig. 1.A, Table ??) with $\eta = 10^{14}$ Pa s and ~~$C^{0*} = 11$~~ $C^{0*} = 10$ for the Gaussian bed topography test case (~~the results are shown in~~ Fig. 4). ~~This qualitatively~~ Bed topography perturbations on the order of 200 m occur commonly (Morlighem et al., 2017a), but inferred slip ratios away from ice steams in the western Greenland ablation zone are typically less than ~ 10 (Morlighem et al., 2013; MacGregor et al., 2016). Thus Fig. 4.C indicates that in these flow conditions ~~unless~~ unless there are exceptionally large C^* ~~perturbations are very large perturbations (on the order of 1000)~~, the ice surface ~~response to expression from~~ C^* perturbations is will be of much smaller amplitude and more disperse than the surface ~~response expressions~~ that can arise from reasonable amplitude bed topography. ~~Since the predicted surface effects from C^* perturbations are generally relatively small in the range of ice flow conditions we are interested in~~ Accordingly, we assume spatially constant C^* (so $C^* = C^{0*}$ at all locations) for all of our analysis.

We next assess the uniqueness ~~with which of~~ C^{0*} and η ~~can be inverted for inversions~~ using the transfer functions. ~~We do this~~, by minimizing misfit (defining misfit % as $100 \frac{(Z-Z')}{\text{Range}(Z)}$) between observed and bed topography transfer predicted ice surfaces (Example inversion results are shown in Fig. 5). ~~We do this over~~ Over our seven study regions of the GHS Greenland Ice Sheet ablation zone (Fig. 1.A, Table ??), ~~and find that in regions with good conditions for applying the transfer functions (where bed DEM error is low and ice velocity is near-uniform), the~~ the values of viscosity that produce best fits between predicted and observed ice surfaces are within half an order of magnitude of 10^{14} Pa s, ~~and the best fitting values of C^{0*} are between 8 and 20~~. For all further analysis we fix the value of η to 10^{14} Pa s, which is within the ~~realm of commonly assumed values of ice viscosity (Cuffey and Paterson, 2010). Except where otherwise noted we fix the value~~ range of ice viscosity estimates (Cuffey and Paterson, 2010).

The best fitting values of C^{0*} ~~to 11, which is also similar to~~ in our study regions range between 6 and 35, and are often not very tightly constrained. Some of these values are significantly higher than other ice sheet ablation zone estimates (Morlighem et al., 2013; MacGregor et al., 2016). ~~We note that~~ Such anomalously high C^{0*} ~~only affects the amplitude of~~ values are not unexpected, for at least two reasons. The first is poor effective bed DEM resolution in some regions, which could result in transfer amplitudes (and thus basal sliding) needing to be artificially high to produce observed surface topographic relief. In regions with lower mean bed DEM error, our inversions result in lower values of sliding (Table ??). The second reason is that the Newtonian rheology used to derive the analytical transfer functions produces generally lower transfer amplitudes than are found with a more realistic (power law) ice rheology (Raymond and Gudmundsson, 2011), so artificially high basal sliding values are needed to produce observed transfer amplitudes. Except where otherwise noted we therefore set $C^{0*} = 10$, which is consistent with the linear transfer functions and likely over-predicts true average slip ratios. Much of our analysis will focus on the wavelengths at which bed topography transfer peaks and not the wavelengths over which these peaks occur (, which are relatively insensitive to the value of C^{0*} . This is because C^{0*} affects transfer peak amplitude but not wavelengths (as can be seen in Fig. 3), so though C^{0*} is likely variable between regions this variability will not affect much of our analysis.C); for parameters representative of our study regions a significant peak is still predicted as long as $C^{0*} > \sim 2$.

2.3.4 Bed DEM error analysis

A significant source of error in our bed topography transfer function method is bed DEM accuracy. The ~~bed DEMs we use have corresponding error maps which represent~~ BedMachine v3 bed DEM has a corresponding potential error map which represents the uncertainty in bed ~~elevation values (elevations (shown in Fig. 82.A)). This uncertainty is primarily a result of incomplete~~
5 ~~primarily reflects poor~~ radar transect coverage, requiring bed elevation in between transects to be modeled. Bed DEM error in this dataset generally depends upon ice velocity and distance from radar transects (Morlighem et al., 2014, 2015). We test the sensitivity of our transfer function to potential bed DEM error by injecting and generally increases with distance from the nearest radar data, but also depends on uncertainty in other data used for mass conservation modeling (Morlighem et al., 2014, 2017a). We use many randomly generated possible error configurations to quantitatively bound the variation in our ice surface
10 topography predictions that is allowed by bed DEM uncertainty. This allows us to assess the robustness of our surface predictions, and to examine the bed DEM accuracy needed for reasonable predictions.

We pseudo-randomly generate 100 randomly generated possible error configurations at for each of 100 different bandpass filter wavelengths λ_n spanning (where λ_n spans the range of wavelengths resolvable in a given domain each domain). Each error configuration is created by using a from a different pseudo-random number generating algorithm to create a complex
15 wavenumber matrix. Each wavenumber matrix has The matrices have the same dimensions as the bed DEM, and has left-right mirrored halves such that real components are symmetric and imaginary components are symmetric real components, and anti-symmetric (where all real and imaginary components vary between -1 and 1) imaginary components. Each wavenumber matrix is then bandpass filtered by multiplication with a narrow Gaussian ring surface (a radially symmetric surface centered around zero wavenumber that along any radial transect is a Gaussian function centered at radius multiplied with a frequency
20 domain Gaussian bandpass filter centered at frequency $\frac{1}{\lambda_n}$). An inverse DFT is then taken of each wavenumber matrix to create pseudo-random surfaces with amplitude spectral peaks at an error surface containing primarily topographic wavelengths near λ_n . Each error surface is then scaled so that all values vary between -1 and 1, and then multiplied by the bed DEM potential error map to generate a possible error configuration. We then add each error configuration to the bed DEM and implement the
25 use bed topography transfer function on each error-injected bed DEM, storing the surface prediction values from each error configuration. By using many randomly generated possible error configurations at a variety of wavelengths, we can assess the range of surface topography variation that is allowed by current bed DEM data quality functions to predict the ice surface over each resulting error-injected bed DEM.

2.3.5 Observed admittance of ice surface/bed topography

Given both bed and surface DEMs, we can calculate the spectral frequency domain admittance of bed topographic features
30 to ice surface topography. Admittance is given by $\hat{A}(k_x, k_y) = \hat{Z}(k_x, k_y) / \hat{B}(k_x, k_y) \hat{Y}(k_x, k_y) = \hat{Z}(k_x, k_y) / \hat{B}(k_x, k_y)$, so if surface topography is were only caused by bed topography transfer then admittance should this admittance should closely correspond to the bed topography transfer function. However, limited DEM precision makes interpreting direct admittance computations and comparing them to transfer functions due to the noise present in 2D admittance computations, interpreting

them directly is challenging. We thus employ two methods to examine admittance. One method is to take 2D discrete Fourier transforms (DFTs) of mirrored and tapered ice surface and bed DEMs (as described in Section 2.3.2), bin and average ~~them~~ the DFTs by absolute wavenumber, then divide the binned wavenumber spectra to obtain 1D admittance. This method ~~thus blends~~ considers both ice-flow-parallel and non-ice-flow-parallel topographic ~~features~~ wavelengths, which could ~~mute the decrease the~~ resulting admittance relative to admittance ~~purely along ice flowlines~~ expected purely in the ice flow direction (since transfer should be highest for topographic wavelengths aligned in this direction). The second method is to interpolate bed and surface elevations along a series of parallel ice flowlines, mirror and taper each flowline elevation profile, take DFTs of each ~~bed~~ profile, then bin and average the wavenumber spectra of all ~~bed~~ profiles. The ~~same is done with ice surface elevation profiles, then the~~ binned ice surface spectra is divided by are then divided by the binned bed spectra to obtain average flowline 1D admittance.

10 This method thus avoids the non-ice-flow-parallel muting effect from the first method, but does not account for the effects of surrounding 2D topography on each flowline (as discussed in Section 2.3.2).

2.4 ~~Meltwater~~ Supraglacial meltwater routing and thermal-fluvial incision

2.4.1 ~~Supraglacial stream network extraction~~ Mechanics of fluvial incision

In terrestrial settings, bedrock fluvial incision is often modeled by the “stream power” law (Seidl and Dietrich, 1992). This model can be combined with another semi-empirical relation Hack’s law (Hack, 1957), relating downstream distance to accumulated flow area. This permits prediction of surface lowering by fluvial erosion E of the substrate at point s along a stream channel downstream of a drainage divide at time t

$$E(s, t) = K(s, t) A(s, t)^m \left| \frac{\partial Z(s, t)}{\partial s} \right|^n, \quad (7)$$

where $A(s, t)$ is accumulated drainage area, $K(s, t)$ is an experimentally determined erodibility coefficient that may vary in space and time, m and n are empirically determined exponents, and $Z(s, t)$ is channel elevation. This model, combined with models for tectonic uplift or hillslope creep, well-predicts large-scale features of many fluvially-dominated terrestrial landscapes. Commonly observed concave-up longitudinal stream elevation profiles and negative slope-drainage area trends are generally interpreted in the context of equation 7, which then may inverted for tectonics and climate, or used to constrain substrate properties such as erodibility K (Gilbert, 1877; Whipple and Tucker, 1999; Montgomery, 2001). Convexities such as those induced by base level changes, non-uniform uplift, and variable climate or substrate properties propagate upstream as kinematic waves (Whipple and Tucker, 1999; Royden and Perron, 2013; OHara et al., submitted 2018).

In supraglacial environments fluvial incision occurs by melting, and an analog of the stream power law may be derived with $n = 1$ (Karlstrom and Yang, 2016). If surface motions introduced by ice advection (analogous to unsteady and non-uniform uplift) are accounted for, fluvially-dominated supraglacial stream profiles with fixed terminal elevations (such as supraglacial lakes) should still approach a concave-up configuration if thermal-fluvial erosion outpaces ice advection (Karlstrom and Yang, 2016). Equation 7 also implies that for fluvially-dominated stream profiles without fixed terminal elevations (such as those flowing into moulins), convexities can progressively propagate upstream from the moulin causing persistent transient topography.

Indeed, convexities at various scales are readily visible in supraglacial stream elevation profiles (see supplement), but these deviations from idealized longitudinal profiles could arise from other processes as well. Spatially varying background ice flow, kinematic waves transmitting uplift or erosion transients (such as from unsteady surface melting or supraglacial lake drainage (Hoffman et al., 2011)), transient surface waves caused by ice flux variations (van de Wal and Oerlemans, 1995), and/or deviations of the local ice velocity vector from the direction of stream flow (such as from stream meanders, e.g., Karlstrom et al., 2013) could all generate convexities in fluviially-dominated supraglacial stream profiles. Alternately, if thermal-fluvial incision is slow enough relative to ice advection and/or other surface processes, stream profiles might not be primarily controlled by fluvial incision, and instead would conform to the shape of the surrounding topography that is controlled by other processes.

Modeling the dynamic interaction between thermal-fluvial incision and ice advection is beyond the scope of this work, and such modeling would still be limited by the resolution of current bed DEMs that affects our transfer function implementation (e.g., Sections 2.1, 2.3.4, and 3.1). We thus instead employ two empirical approaches to search for signatures of IDC-scale landscape modification by thermal-fluvial incision, and to quantify the observed pattern of supraglacial stream networks in relation to bed topography transfer. The first approach is to compare slope versus accumulated drainage/flow area relations, a traditional terrestrial landscape metric (Gilbert, 1877; Whipple and Tucker, 1999; Montgomery, 2001), between real supraglacial stream networks and synthetic flow networks calculated on bed topography transfer predicted surfaces (described in Section 2.4.3). The second approach is to use two stream conformity metrics to quantify how well supraglacial stream network geometry is explained by the surrounding ice surface topography filtered at various wavelength thresholds (described in Section 2.4.4).

2.4.2 Supraglacial stream network and synthetic flow network extraction

We use satellite imagery, DEMs, and ~~flow-routing-flow-routing~~ algorithms to extract supraglacial stream networks from seven regions of the western ~~GIS Greenland Ice Sheet~~ ablation zone (Karlstrom and Yang, 2016; Yang and Smith, 2016)(~~Fig. 6~~). Satellite imagery is used to identify ~~by-hand-moulins/lakes~~moulins by hand, which are treated as water sinks. We then use ~~flow-routing-flow-routing~~ to calculate accumulated flow/drainage area patterns on the surface ~~-(as shown in the example stream network in Fig. 6.A)~~. We use the D8 (steepest descent) ~~flow-routing-algorithm-from-ArcGIS~~ flow-routing algorithm with channel area threshold set to maximize agreement with visible stream channels, between 8000 and 30000 m² depending upon region. In general, ~~flow-routing-flow-routing~~ is an imperfect means of finding real stream channels, especially on a relatively flat landscape such as the ~~GIS Greenland Ice Sheet~~. DEM resolution is not high enough to resolve narrow (< ~2 m wide) supraglacial stream channels, so such streams may be missed by ~~flow-routing-flow-routing~~, particularly those that are not aligned with the steepest descent direction (Smith et al., 2015; Yang et al., 2015). However, most streams found via our ~~flow-routing-flow-routing~~ method agree with visually identified stream channels (~~Karlstrom and Yang, 2016; Yang and Smith, 2016~~) (Yang and Smith, 2016).

~~We employ two approaches to quantify the observed pattern of supraglacial stream networks in relation to ice flow and bed topography transfer. The first approach is to compare slope versus accumulated drainage/flow area relations (a traditional terrestrial landscape metric (Gilbert, 1877; Whipple and Tucker, 1999; Montgomery, 2001)) between real supraglacial stream~~

~~networks and~~ Bed topography transfer provides a way of constructing synthetic flow networks ~~on surfaces without streams~~ (either stream-free regions of the GIS or bed topography transfer predicted surfaces). The second approach is to quantify how well supraglacial stream network geometry is explained by the surrounding ice surface and what topographic wavelengths are most important for this.

5 ~~We create synthetic flow networks in two ways. We first compute synthetic flow pathways on a stream-free region of the GIS by placing artificial moulins (as water sinks) at the base of large depressions, then predicting flow pathways numerically. This method is complicated by the presence of few regions of the GIS differing only in the presence or absence of~~ to examine how meltwater would route in the absence of supraglacial thermal-fluvial incision, ~~and since moulins do not only occur in depressions (Catania et al., 2008; Yang et al., 2015; Yang and Smith, 2016). Bed topography transfer provides another way to~~
10 ~~construct synthetic stream networks since incision is not accounted for by the transfer functions.~~ We use transfer functions to predict the ice surface over bed DEMs, then place artificial moulins as water sinks at the base of large surface depressions and calculate synthetic flow networks numerically. ~~We calculate all~~ These are not perfectly comparable with real supraglacial stream networks, since moulins also occur outside of depressions (Catania et al., 2008; Yang et al., 2015; Yang and Smith, 2016). We calculate these synthetic flow networks with the TopoToolbox (Schwanghart, 2014) D8 method, with channel area threshold
15 set to 20000 m².

2.4.3 Slope versus Supraglacial stream network slope and accumulated drainage area and thermal-fluvial incision relations

Our first approach for quantifying controls on meltwater routing comes from the hypothesis that bed topography transfer can explain ~~meltwater routing trajectories~~ supraglacial stream longitudinal elevation profiles, without appealing to ~~fluvial incision.~~
20 ~~If significant landscape shaping by thermal-fluvial incision. Although modeling the transient competition between ice flow over bed topography and thermal-fluvial incision is outside the scope of the present work, if bed topography transfer is the dominant process then slope-drainage relations on synthetic flow networks will match those from observed supraglacial stream networks. If instead~~ supraglacial stream incision is a primary control on ice surface topography at km scales, the interplay between thermal-fluvial erosion and ice flow will set the longitudinal profiles of streams and the relationship between slope and
25 accumulated ~~flow/drainage area of streams networks (Karlstrom and Yang, 2016)~~ observed stream networks may consistently differ from synthetic flow networks.

~~Modeling the transient competition between ice flow and thermal-fluvial incision is outside the scope of the present work. Instead, we use empirical metrics to compare the relation of slope to~~ We compare local channel slope to local accumulated upstream flow/drainage area at all points in each stream network. Prior to doing this we smooth all stream longitudinal profiles
30 to remove small-scale slope variations. Profile smoothing is done by first breaking each stream network into multiple separate stream profiles, discarding all profiles less than 800 m long, then twice applying a moving average filter with a span of 200 m (analogous to a lowpass filter ~~with a 200-m wavelength threshold~~) to each remaining profile, and finally trimming 100 m from both ends of each profile to remove smoothing-induced edge effects. We then calculate stream longitudinal slopes with a ~~2nd~~ second order centered finite difference ~~approximation~~ stencil. There is a large scatter in the resulting slope versus drainage area

relations, so for each stream network we divide data points into logarithmically spaced area bins and calculate the **average slope mean and standard deviation of slopes** in each bin (Montgomery, 2001; Warren et al., 2004).

2.4.4 Supraglacial stream network topographic conformity

Our second approach for quantifying **controls on** meltwater routing is to implement two **regional** measures of stream network conformity to surrounding ice surface topography **devised by**, **as in** Black et al. (2017). This approach assesses the degree to which stream patterns are “explained by” the current configuration of surrounding ice surface topography at various wavelengths. Percent downhill ($%d$) measures the percentage of the length along stream channels over which the streams are flowing downhill. **Conformity**, **and conformity** factor (Λ) measures the mean deviation of stream channel paths from the direction of steepest descent on the ice surface **(as illustrated in Fig. 6.B)**. We low-pass filter ice surface DEMs using a series of decreasing cutoff and taper wavelengths, then calculate **percent downhill and stream conformity factor** $%d$ and Λ by projecting stream networks onto each filtered surface **(as illustrated in Fig. 6.B)**. **We note that applying these conformity metrics to stream networks calculated with flow-routing may result in a bias towards artificially high conformity, since as mentioned in Section 2.4.2 flow-routing on imperfect DEMs may miss some narrow stream channels that are not aligned with the steepest descent direction on the ice surface. However, our flow-routing is done on sufficiently high-resolution DEMs to correctly capture the majority of observed stream network structures.**

As filter cutoff wavelength decreases, both conformity metrics will increase if stream network geometry is controlled by the progressively shorter wavelengths of topography that are being included (Black et al., 2017). With a perfect DEM, as filter cutoff wavelength approaches zero $%d$ should generally increase and approach 100% since streams do not flow uphill. Similarly, Λ should generally increase and approach 1, since water should generally flow in the direction of steepest descent.

As filter cutoff wavelength increases both metrics will decrease if stream network geometry is controlled by the shorter Stream network structure might depend on particular wavelengths of topography **that are being removed (Black et al., 2017)**. **Such decreases in conformity might occur** for a variety of reasons, for example if **the wavelengths being removed those wavelengths** encompass topographic features that predate stream formation and thus contributed to the routing of the stream channel when it formed. **Conformity decreases could also occur at longer cutoff filter wavelengths if fluvially driven stream channels when they formed. Alternately, stream networks might not perfectly conform to the surrounding longer wavelength topography if fluvial** meanders have shifted channels away from the **background** direction of steepest descent **relative to background topography**, or if **background the surrounding** topography has been modified **post stream-incision** by processes such as ice advection (Black et al., 2017; Wegmann et al., 2007). **We (e.g., for tectonic processes, Black et al., 2017; Wegmann et al., 2007)**. **We do not focus on why stream network conformity might be imperfect at any given wavelength, but instead** use the conformity metrics **only** to indicate what topographic wavelengths are important for explaining current supraglacial meltwater routing.

To calculate the two conformity metrics, we **low-pass filter ice surface DEMs using one-sided Gaussian filters. Prior to filtering we** apply pre-processing steps as described in Section 2.3.2 to minimize edge effects, **then low-pass filter ice surface DEMs using one-sided Gaussian filters.** We then project flow networks (as **found computed** on the unfiltered DEMs) onto

~~the filtered surfaces. Each filtered surface (as illustrated in Fig. 6). We calculate %d as the percent of discrete locations along stream channels that are higher in elevation than the next downstream locations along the same channels location. To calculate Λ , at each discrete location along a stream we calculate the angle between the horizontal direction vector of the stream channel (the direction water is flowing) and the horizontal direction vector of steepest descent down the ice surface. Λ is then given by the mean absolute value of the cosine of this angle at all discrete stream channel locations. Exact expressions for %d and Λ are given in Appendix ??.~~ We note that applying these conformity metrics to stream networks calculated with flow routing on imperfect DEMs may result in a bias towards artificially high conformity, since as mentioned in Section 2.4.2 flow routing may miss some narrow stream channels that are not aligned with the steepest descent direction on the ice surface. However, since we have verified that flow routing properly captures the majority of stream network structure we expect that the general trends in conformity metrics observed with changing filter wavelengths will be valid. the supplement.

2.5 Identifying ice surface Predicting supraglacial topographic drainage basins and subglacial hydraulic flow pathways

~~We are interested in examining the response of IDCs to changing ice flow conditions using bed topography transfer predictions.~~ Bed topography transfer functions provide a tool for examining the effects various multiple-year averaged ice flow parameters have on ice surface topography. To do this we ~~extract topographic basins from predicted first predict ice surface topography (as described in Section 2.3.2) over one example study region R1 (Fig. 1.A, Table ??) with various ice flow and basal sliding parameters in a given region with different ice flow parameters.~~ We can then explore the effects these changes in surface topography might have on both supraglacial and subglacial hydrology.

To examine potential changes in supraglacial hydrology, we delineate surface topographic drainage basins on the predicted ice surfaces. We do this using flow-routing (with all topographic local minima treated as water sinks, as described in Section 2.4.2) to identify topographic drainage basin divides, counting all edge terminating basins separately. Topographic basins will not exactly correspond to IDCs, since moulins fragment topographic basins and/or there could be places where streams have incised through topographic divides (Smith et al., 2015; Yang et al., 2015; Yang and Smith, 2016), but in (Yang et al., 2015). In practice there is a reasonable correspondence between topographic basins and IDCs. ~~We use flow routing as described in Section 2.4.2, with all topographic local minima treated as water sinks, to identify basin divides. All edge terminating topographic basins are counted separately. if appropriate DEM processing is used (Yang and Smith, 2016), so this approach provides a reasonable indication of how IDC configuration and number density would vary with changing multiple-year averaged ice flow parameters.~~

To explore potential changes in subglacial hydrology that might arise from changing ice flow conditions, we model quasi-static water flow patterns under the predicted ice surfaces. We first calculate subglacial hydraulic potential ϕ_h as a function of relative bed elevation and ice thickness following Hewitt (2011)

$$\phi_h(x, y) = \rho_w g B(x, y) + \rho_i g H(x, y) \left(\frac{P_w}{P_i} \right) \quad (8)$$

where $\frac{P_w}{P_i}$ is the ratio of basal water pressure to ice overburden pressure. We assume basal water pressure is equal to ice overburden pressure everywhere, in order to estimate the maximum possible impact of surface topography on subglacial hydraulic potential. Subglacial water is often modeled as flowing down gradients in hydraulic potential (Hewitt, 2011; Wright et al., 2016). We thus apply flow-routing to the hydraulic potential fields to determine water flow paths and create accumulated flow/drainage area maps. We first fill sinks (local minima) in the hydraulic potential field in order to force all water to flow out of the domain. We then apply a multi-direction flow-routing algorithm from TopoToolbox (Schwanghart, 2014) since this produces more realistic flow pathways than D8 flow-routing in low-gradient areas (Quinn et al., 1991). We cannot account for water flow into the domain from up-gradient regions with this approach, so the drainage areas we calculate are lower bounds. These simple calculations also do not account for many important factors influencing subglacial hydrology such as basal melting/freezing, permeability, and subglacial channelization (Rempel, 2009; Schoof, 2010; Sole et al., 2011; Werder et al., 2013; Chandler et al., 2013), nor do they account for variation of flow pathways on timescales that differ from ice flow changes. However, they provide a useful tool for exploring the sensitivity of subglacial hydrology to the perturbations in surface topography caused by changing multiple-year averaged ice flow parameters.

3 Results

3.1 Bed topography transfer

We calculate observed admittance of bed topography to ice surface topography (as described in Section 2.3.5) in ~~the our~~ seven study regions ~~of the western GIS on the western Greenland Ice Sheet~~ ablation zone. In all regions, admittance corresponds well to predicted bed topography transfer amplitudes (as described in Section 2.3.1) at wavelengths $> \sim 1$ km. ~~Results are shown in~~ Fig. 7). Notably, admittance peaks appear at wavelengths from ~ 1 -10 km, as predicted by bed topography transfer functions. ~~We expect that calculated admittance at wavelengths < 1 km often appears higher than predicted in part due to limited effective bed DEM resolution at these shorter wavelengths, and in part due to other processes creating short-wavelength surface topography (such as fluvial incision). That there is good agreement between the transfer functions and calculated admittance at wavelengths $> \sim 1$ km provides one piece of evidence that bed topography transfer is a dominant control on surface topography at these scales.~~

We then use the steady-state bed topography transfer functions to predict ~~the ice surface~~ ice surface topography (as described in Section 2.3.2) in our seven study regions (Fig. 1.A, Table ??). ~~We find that~~ Example results from region R1 are shown in (Fig. 8). ~~In regions R1, R2, and R7 the transfer functions accurately predict surface relief and~~ qualitatively well predict general IDC-scale (~ 1 -10 km, consistent with our admittance calculations) features of the ice surface, such as large ridges and depressions (see Fig. 8) ~~A.B and supplement). In regions R3, R4, R5, and R6 the transfer functions significantly "under-predict" surface topography by creating noticeably smoother surfaces than observed. We expect that this is primarily due to the limited effective bed DEM resolution in these regions, as discussed below.~~

~~Admittance in all regions exhibit a significant discrepancy from bed topography transfer predictions at wavelengths $< \sim 1$ km (Fig. 7). Misfit between the~~ Even in regions where predictions are qualitatively good, misfit between bed transfer predicted

ice surfaces and ice surface DEMs is ~~also often non-trivial~~often significant, with mean misfit values of ~~~8-169-14%~~ of the surface topographic relief in each region (~~see example misfit map in~~ Fig. 8.C, and data from all study regions in Table ??). As discussed in ~~sections 2.3.1~~Sections 2.3.1 and 2.3.2, there are many potential causes of ~~these discrepancies including such misfit~~: bed DEM error, the various assumptions made in deriving and implementing the transfer functions (such as assuming
5 Newtonian ice rheology, linearity, and a steady-state limit), and/or unaccounted for physics.

We use the approach described in Section 2.3.4 to examine the potential effects of bed DEM error on ice surface predictions in our study regions, ~~and find that the potential effects of bed DEM error on ice surface predictions are~~. This can be significant, ranging from ~40% to larger than 100% of regional ice surface relief depending upon the configuration and magnitude of DEM error. However, where bed DEMs are relatively accurate (generally less than ~~~100 m~~60-100 m potential error) these
10 error effects are smaller than the regional ice surface relief (~~as shown in~~ Fig. 8.D), indicating that ~~at least~~large-scale features of surface predictions in these areas ~~are meaningful despite bed DEM error. Unfortunately bed data error is~~ should be meaningful. Unfortunately potential bed DEM error is currently worse than 100 m over much of the GIS (Morlighem et al., 2014, 2015; ?), making detailed Greenland Ice Sheet (Morlighem et al. (2017a, b), Fig. 2), limiting the possible precision of surface predictions or inversions for parameters like basal sliding (C^*) ~~unreliable~~in many regionswith current data. We only use surface predictions
15 from study regions R1 (shown).

~~Thus we have shown that, where bed DEMs are sufficiently accurate, bed topography transfer can explain IDC-scale (~1-10 km) ice surface amplitude spectra and IDC-scale ice surface topographic features. This provides verification that bed topography is a dominant control on IDC scale surface topography, though with insufficient resolution to directly quantify the significance of other processes like thermal-fluvial incision that are superimposed on the effects of bed topography.~~

20 3.2 Supraglacial stream network slope and accumulated drainage area relations

Supraglacial stream networks from our seven study areas (Fig. 1.A, Table ??) all exhibit negative slope versus drainage area relationships (thus positive concavity), as shown in Fig. 9. This is expected in a fluvially controlled landscape (as discussed in Section 2.4.3, or see Montgomery (2001)). However, negative slope-area relations can arise without fluvial incision in randomly generated DEMs (Schorghofer and Rothman, 2002), so in isolation this geomorphic metric is challenging to invert uniquely
25 for process. We thus use control cases with no fluvial influence for comparison; these controls are synthetic flow networks created by artificially placing moulins on bed topography transfer predicted ice surfaces (as described in Section 2.4.2). The map-view structure of synthetic flow networks is not realistic, since the bed topography transfer predicted surfaces are very smooth and D-8 flow-routing then produces straight and parallel channels. However, in slope-drainage area space, synthetic flow networks in regions with qualitatively reasonable surface predictions (R1, R2, and R7) exhibit similar negative slope-area trends to the corresponding observed stream networks, as shown in Fig. 9. The slope area trends of regions R3, R4, and R5 are noticeably flatter than the corresponding observed stream networks. We expect this is mainly because limited effective bed DEM resolution results in under-predicted surface topography, on which all surface slopes deviate minimally from the regional background slope (α).
30

In regions with more reliable surface predictions (R1, R2, and R7), synthetic and observed slope-area trends have similar slopes as shown by the power-law fits in Fig. 8) and 9. In the absence of additional physical processes besides erosion, the power-law leading coefficient would be expected to correspond to K/n and the exponent to correspond to m/n from equation 7. There are deviations between observed stream networks and synthetic flow networks in regions R1, R2 in the following meltwater routing analysis, and R7, but there is not a clear consistency in such deviations between these regions. Given the very large scatter inherent to slope-area relations (shown in Fig. 9 and discussed by Warren et al. (2004)) and the limitations of our surface predictions, it is difficult to say from this data if there are consistent slope-area discrepancies that could indicate a fluvial signature in observed stream networks. Further study with better bed DEMs and more detailed ice flow modeling might tease out such fluvial signatures. However, our results are sufficient to show that given accurate enough bed DEMs, bed topography transfer alone can produce synthetic stream networks with longitudinal slope-area structure approximately similar to observed stream networks.

3.3 Meltwater routing Supraglacial stream network topographic conformity

3.3.1 Supraglacial stream network topographic conformity

We apply We calculate both stream network topographic conformity metrics (as described in Section 2.4.4 to) for supraglacial stream networks from our seven study regions (Fig. 1.A, Table ??), and to synthetic flow networks from a non-fluvially-iceised region and from two bed topography transfer predicted ice surfaces (in study regions R1 and R2). We find; results are shown in Fig. 10. In all regions there are consistent trends in both $\%d$ (percent downhill) and Λ (conformity factor) for all stream and synthetic flow networks (Fig. 10). At the longest wavelength cutoffs $\%d$ and Λ are at their lowest regional values, and including shorter topographic wavelengths generally results in increases in both metrics. $\%d$ and Λ plateau at values between 88–97% and 0.75–0.81 respectively, except for in synthetic flow networks calculated on bed topography transfer predicted surfaces, where the metrics approach the expected maximum $\sim 88–97\%$ and $\sim 0.75–0.81$ respectively. That these values plateau at less than the maximum respective values of 100% and 1. The lower plateau values observed and 1 in real stream networks could be caused by due to varying channel depths and/or DEM inaccuracy; we normalized the values of both metrics in Fig. 10 to better highlight how the metrics change from their plateau values as progressively longer topographic wavelengths are removed.

Significantly, in all stream and synthetic flow networks, In all stream networks changes in both $\%d$ and Λ occur in bands of cutoff wavelengths roughly between 1 and 10 km. This indicates that these wavelengths of topography explain the general are the wavelengths that are most important for explaining the overall structure of supraglacial stream networks. These wavelength bands generally match the peaks in match the wavelengths at which predicted bed topography transfer predicted wavelengths (is highest, and also where we find peak admittance between surface and bed DEMs (see Fig. 7). In particular, we note that the region where stream conformity is more affected by smaller wavelengths (solid red curves) would be expected to exhibit comparatively high bed topography transfer at these smaller wavelengths. The regions where stream conformity is less effected

by smaller wavelengths (solid yellow, green, and purple curves) would be expected to exhibit comparatively low bed topography transfer at these wavelengths. This is consistent with empirical admittance calculations in Fig. 7.

3.3.1 Supraglacial stream network slope versus drainage area and thermal-fluvial incision

Individual supraglacial stream elevation profiles exhibit many readily visible deviations from idealized concave up longitudinal profiles (as described in Section 2.4.3) (Fig. 6). Supraglacial stream networks from our seven study areas (Fig. 1.A, Table ??) all exhibit negative slope versus drainage area relationships (thus positive concavity), as might be expected from fluvial control (Fig. 9). However, we also find negative slope-area trends in synthetic flow networks created by flow routing on an area of the GIS with no significant thermal-fluvial incision, and on two bed topography transfer-predicted surfaces (from study regions R1 and R2). This is consistent with previous work showing that negative slope-area relations can arise even in randomly generated topography (Schorghofer and Rothman, 2002), making this often-used geomorphic metric challenging to invert uniquely for process.

Though the synthetic flow network slope-area trend from one supraglacial stream network (SN-R2) appears appreciably steeper than the corresponding synthetic flow network on a bed topography transfer-predicted surface (FN-BTT-R2), overall the slope-area trends in synthetic flow networks appear to be similar to those on fluvially incised regions of the real ice surface, given the inherent scatter of slope-area relations (Warren et al., 2004). Further stream network data could allow for a finer distinguishment of slope-area relations between IDCs, but from these results it seems that bed topography transfer is sufficient to explain supraglacial stream longitudinal elevation profiles on at least ~ 1 -10 km scales, independent of thermal-fluvial incision. Thus in all of our study regions the general routing of surface meltwater according to these conformity metrics is consistent with control by bed topography.

4 Discussion

Our observations indicate that in regions of the GIS ablation zone with near-uniform ice velocity, given ice flow conditions (including basal sliding) our combined results thus demonstrate that given sufficiently accurate bed DEMs, bed topography transfer alone can explain reasonably well explain ablation zone IDC-scale (~ 1 -10 km scale ice sheet surface topography). Given moulin locations (which dictate where water leaves the surface environment), bed ice surface topography also explains both stream network conformity metrics and stream network slope-area relations. We thus propose that bed topography transfer can explain the and meltwater routing. This conclusion is supported by surface topographic admittance calculations, bed transfer predictions of surface topography, and three different geomorphological metrics of supraglacial stream network structure. This suggests that the effects of thermal-fluvial incision on IDC-scale (~ 1 -10 km) structure of supraglacial meltwater routing are secondary, superimposed on the dominant basal control of surface topography.

4 Discussion

4.1 Predicting supraglacial IDC evolution

Given moulin locations and ice flow conditions, our results imply that bed topography transfer should generally explain IDC configurations, such as the trend observed by Yang and Smith (2016) where average IDC area increases with increasing ice surface elevation/thickness. ~~It is~~The bed topography transfer functions also provide a tool to perform a parameter study and predict IDC-scale surface topography under different long-term averaged ice flow conditions. Even without predicting moulin locations, we can still use our methodology to examine the general response of surface topographic basins to changing ice flow conditions as described in Section 2.5. This is important since surface topography and IDC configuration could impact subglacial hydrology, as we discuss in the next section (Section. 4.2). Additionally, it is expected that the ablation zone of the GIS Greenland Ice Sheet will move to higher elevations in ~~the coming years~~coming years as global climate warms (Rae et al., 2012; Fettweis et al., 2013; Leeson et al., 2015). ~~The method we have developed provides a tool to predict how the large scale structure of ice sheet surface drainage will respond to changes in ice flow and/or basal sliding, as might be expected to occur in the future. If moulin locations could also be predicted, this knowledge could then~~Given moulin locations, an approach similar to what we implement here could be used to ~~predict the~~obtain precise predictions of the of the spatial and temporal input of surface meltwater into moulins ~~with methods~~if combined with tools such as empirically calibrated hydrographs (e.g., Smith et al., 2017).~~Even without predicting moulin locations, we can still examine the general response of topographic basins to changing ice flow conditions.~~

The topographic basins associated with predicted ice surfaces under varying in different multiple-year averaged ice flow conditions are shown in Fig. 11. ~~As discussed in Section 2.3.1, the timescale over which the ice sheet surface approaches 95% of its steady state configuration in response to a basal perturbation is on the order of 3-60 years depending upon perturbation wavelength (though some adjustment occurs much more rapidly), so our steady state predictions might be better interpreted as multi-year average ice surface configurations. If ice surface adjustments to variable basal conditions or ice flow perturbations are sufficiently rapid, surface topographic basin configuration should also vary on seasonal timescales.~~

~~We again~~We note that topographic basins will not exactly correspond to IDCs (Smith et al., 2015; Yang et al., 2015; Yang and Smith, 2016).~~For~~for comparison we show IDC configurations obtained solely from satellite imagery by Yang and Smith (2016) (in Fig. 11).A. Despite the visible differences between our bed topography transfer predicted topographic basin configuration and the observed IDC configuration, the overall basin ~~IDC~~and IDC number densities are similar. This is consistent with results from Yang and Smith (2016) showing that surface topography roughly predicts IDC configurations. We thus expect ~~that changes in~~ topographic basin density ~~changes~~ predicted with changing ice flow conditions should generally correspond to changes in IDC density. We ~~find~~show in Fig. 11 that changes in ice surface slope α or ice surface velocity U by factors of two do not significantly ~~effect~~affect topographic basin density. However, ~~we find that~~ topographic basin density decreases appreciably with increasing ice thickness, and increases appreciably with increasing basal sliding. Our analysis thus indicates that ice surface topographic basin density in the GIS Greenland Ice Sheet ablation zone could be significantly affected by ~~perturbations to~~changes in long-term averaged ice thickness or basal sliding.

4.2 Coupling between supraglacial IDC density and subglacial hydrologic regime

As discussed in Section 2.3.1, the timescale over which the ice sheet surface approaches 95% of its steady state configuration in response to a basal perturbation is on the order of 3–60 years depending upon perturbation wavelength, so the results here (and in the following Section 4.2) should be interpreted as predicting multiple-year averaged ice surface configurations. Minimal adjustment to changing ice flow or basal sliding conditions is predicted on shorter seasonal timescales, although increasingly high temporal resolution observations could motivate such shorter timescale modeling in the future.

~~Basal sliding can change significantly on timescales as short as hours (Selmes et al., 2011; Sole et al., 2011; Chandler et al., 2013; Shannan et al., 2013) and is also the parameter that most significantly affects surface topographic basin density (~~

4.2 Potential coupling between ice surface topography and subglacial hydrology

We have shown in Section 4.1 that changing ice flow conditions should result in changing ice surface topography and supraglacial IDC configuration (see Fig. 11); we can now explore and speculate upon how such changes might affect subglacial hydrology and/or basal sliding.

Perturbations to surface topography could have direct impacts on subglacial hydraulic potential, and thus on subglacial water flow pathways. We calculate such pathways as described in Section 2.5; the results are shown in Fig. 12. The predicted variations in subglacial meltwater flow patterns are subtle, but there is some change in all cases. This is most visible where the configuration of high-flow-area paths changes, as can be seen near the center of the study region between Fig. 12.B5 and Fig. 12.B6. The threshold flow-area we use to calculate areal percentages in Fig. 12 ($5 \times 10^6 \text{ m}^2$) was chosen to highlight pathways of high relative flow area. Subglacial channelization (discussed more later in this section) should occur preferentially around such pathways, since water flux should generally increase with increasing flow area (Hewitt, 2011; Wright et al., 2016). Doubling C^{0*} or α slightly increases the percent of the study region covered by such higher-flow pathways, while doubling U or H has the opposite effect. The magnitude of these changes is generally less than around 20% of the baseline areal coverage for any chosen flow-area threshold. Dynamic subglacial hydrology models (such as Schoof, 2010 or Werder et al., 2013) are needed to more completely assess the potential impacts of these changes. However, our results indicate that unless any of the multiple-year averaged ice flow parameters changes by more than a factor of two, the effects (that are directly caused by perturbations in surface topography) such changes will have on subglacial hydraulic pathways are likely to be subtle.

Our calculations suggest that the more important influence of ice surface topography on subglacial hydrology may be from the dispersion of surface meltwater input caused by changing surface topographic basin (or IDC) number density (as shown in Fig. 11). For a given melt production rate, if topographic basin density increases then meltwater input to the subglacial environment will be dispersed among more moulins, up to the point at which some basins become small enough that they fill and overtop without building up enough water pressure to generate moulins through hydrofracturing (Banwell et al., 2012, 2016). This dispersion of moulin water input could impact subglacial hydrology in several ways. If such dispersion results in average subglacial water pressure increases (due to less effective subglacial channelization) as moulin input becomes more dispersed or rapid development of subglacial channels, this could lead to lower average basal effective stresses and thus increases in

increased basal sliding (Werder et al., 2013; Banwell et al., 2016; Hoffman et al., 2018). Alternately, if subglacial channelization happens rapidly regardless of meltwater input rate, then the dispersion of meltwater input may not be particularly significant or may result in more effective subglacial channel networks (Banwell et al., 2016). The extent to which subglacial channelization occurs is debated (Meierbachtol et al., 2013), but some subglacial channelization may occur on timescales of hours to days with continuing evolution over the length of melt seasons, and in the GIS-Greenland Ice Sheet ablation zone moulin meltwater input is a significant source of basal water effecting this subglacial drainage development (Schoof, 2010; Sole et al., 2011; Werder et al., 2013; Chandler et al., 2013). Of course, the total amount and timing of surface meltwater flux will also change if the annual surface energy budget varies (Cuffey and Paterson, 2010; Ahlström et al., 2017), if the average albedo of IDCs varies (Leeson et al., 2015), or if partitioning between slow (porous snow/weathering crust flow, firn aquifer) and fast (stream channel) pathways varies (e.g., Karlstrom et al., 2014; Cooper et al., 2018; Yang et al., 2018). We see including such effects in glacial surface models as a promising avenue for future research.

~~Dispersing water input among more moulins could increase average basal water pressure (thus decreasing basal effective stress and increasing basal sliding) if water flux through each moulin becomes low enough to preclude efficient subglacial channel development. If this occurs, our results imply a positive feedback where increasing basal sliding increases IDC. Basal sliding is the parameter that generally has the most significant effect on surface topographic basin density (as shown in Fig. 11). Basal sliding can change significantly over timescales from hours to years, and often has strong seasonal cycles (Selmes et al., 2011; Sole et al., 2011; Chandler et al., 2013; Shannon et al., 2013). As discussed in Sections 2.3.2 and 2.3.3, the long term averaged basal sliding parameter we assume in implementing basal transfer functions may not directly relate to the real seasonally varying values of basal slip ratio (Tedstone et al., 2014). However, the effects from relative changes in basal sliding that our methods predict should be more robust, and it is reasonable to expect that persistent changes in basal sliding during melt seasons and/moulin density which then further increases basal sliding. This feedback could be shut off by sufficiently decreased melt water production at the surface, by basin density increasing to the point that supraglacial lakes overflow to downslope catchments or do not rapidly build up water pressure for fracturing (Banwell et al., 2012, 2016), and /or by adjustment of other ice flow parameters to increased basal sliding (Hoffman and Price, 2014). Alternately, dispersing subglacial meltwater input among more moulins could result in more efficient subglacial drainage (thus lower basal water pressure and reduced sliding) if there is still sufficient water flux through each moulin to drive efficient subglacial channelization (Banwell et al., 2016). In this case there would be a negative feedback where increasing basal sliding increases IDC /moulin density, which then decreases in the length of melt seasons could have effects on surface topography that are analogous to this long-term averaged basal sliding parameter. Our results thus indicate that there are potential feedbacks wherein changes in long-term averaged basal sliding affect surface IDC configurations, which could in turn affect subglacial hydrology and basal sliding.~~

4.3 Thermal-fluvial incision on sub-IDC scales

~~Modeled melt rates in many areas of the GIS ablation zone are greater than 1 m/yr (water equivalent) (Noel et al., 2015), but the ice surface in these areas can be advecting stream channels horizontally across surface features from basal transfer at velocities~~

greater than 100 m/yr (Joughin et al., 2010b, a; Nagler et al., 2015). Most IDCs on the GIS have maximum dimensions of 1-10s of km (Yang and Smith, 2016). Our admittance calculations indicate that bedrock transfer is less important for Our analysis suggests that the influence of thermal-fluvial incision on large (> 1 km) scale surface topography and stream network structures is superimposed on the dominant influence of bed topography. However, admittance calculations show that other influences on ice surface topography could become more significant at scales < ~1 km (see Fig. 7), and we expect fluvial incision to be a more primary influence on surface topography and meltwater routing pathways on-at these scales. On larger scales, our stream network and synthetic flow network analysis indicates that thermal-fluvial incision is convolved with bed topography controls on stream profiles (Fig. 9).

In terrestrial settings, bedrock fluvial incision is often modeled by the “stream power” law (Seidl and Dietrich, 1992). This semi-empirical model can be combined with Hack’s law (Hack, 1957) relating downstream distance to accumulated flow area to predict surface lowering by mechanical erosion E of the substrate at point s along a stream channel downstream of a drainage divide at time t

$$E(s, t) = kA(s, t)^m \frac{\partial Z(s, t)}{\partial s},$$

where A is accumulated drainage area, k is an experimentally determined coefficient, and m is an experimentally determined exponent.

In supraglacial environments fluvial erosion occurs by melting, but an analog of stream power may be derived (Karlstrom and Yang, 2016). Combined with a model for ice flow along the stream channel (Cuffey and Paterson, 2010), the following general surface evolution equation is obtained

$$\frac{\partial Z(s, t)}{\partial t} = -kA(s, t)^m \frac{\partial Z(s, t)}{\partial s} + f(s, t)$$

where f includes multiple terms that account for substrate movement (surface melting and ice flow) (Karlstrom and Yang, 2016).

In terrestrial settings, concave-up profiles and negative slope-area trends are often observed and interpreted as consequences of fluvial incision, because this is the steady state configuration approached by an erosionally controlled stream profile under uniform uplift (Gilbert, 1877; Whipple and Tucker, 1999; Montgomery, 2001). In the supraglacial environment, this concave-up configuration could be approached by streams with fixed terminal elevations such as supraglacial lakes (Karlstrom and Yang, 2016). Alternately, the erosion equation implies that for streams without fixed terminal elevations, such as those flowing over ice cliffs or into moulins, stream profiles should exhibit pervasive convexities due to transient changes at the boundary that persist through the time period of active incision (the melt season). Convexities induced by base level changes or non-uniform uplift propagate upstream as kinematic waves (Whipple and Tucker, 1999). In supraglacial streams, convexities could reflect such kinematic waves, transmitting impulsive uplift or erosion transients such as unsteady surface melting or supraglacial lake drainage (Hoffman et al., 2011). They might also record transient surface waves caused by ice flux variations (van de Wal and Oerlemans, 2002). Ice flux wave propagation speed likely differs from fluvial knickpoint propagation speed (Karlstrom and Yang, 2016).

In the terrestrial fluvial environment, convexities may also result from temporally steady but spatially variable uplift or substrate erodibility (Royden and Perron, 2013; OHara et al., submitted 2018). In the supraglacial environment, flow over rough bed topography, variable basal sliding or ice rheology, and/or deviations of the local ice velocity vector from the direction of stream flow (which could be caused by stream meanders, Karlstrom et al., 2013) could generate such convexities. If thermal-fluvial incision is slow enough relative to ice advection and/or other surface processes, stream profiles should not be significantly controlled by incision. In this case, channels would instead conform to the shape of the surrounding topography that is controlled by other processes.

Our conformity metric calculations (Fig. 10) are consistent with an external control on supraglacial stream network geometry. However, models that couple transient ice flow over rough bed topography to a surface energy balance, along with accurate bed DEMs, will be necessary to rule out some quantitatively constrain the influence of thermal-fluvial incision on ice surface topography and meltwater routing. Such models are also required to address observed supraglacial channel network coarsening (e.g., Yang and Smith, 2016), (time evolution of channel density, (e.g., Yang and Smith, 2016)), and to establish how diurnally and seasonally varying melt rates are imprinted on stream networks.

From the standpoint of predicting Greenland Ice Sheet-wide hydrology, our work may simplify future modeling efforts. If thermal-fluvial incision does not significantly modify the ice surface at IDC-scales, thermal-fluvial supraglacial stream incision would not need to be fully coupled with ice sheet models in order account for to predict meltwater routing and the general evolution of the ice surface. Rather, future work larger-scale evolution of ice surface topography over long timescales. Future work towards this goal should focus on better predicting transfer of bed topography, basal sliding, and ice flux variations to the surface, and on determining bed elevations and predicting moulin formation. This work is needed to accurately predict the spatial distribution of IDCs through time. (Joughin et al., 2013; Young et al., 2018).

5 Conclusions

Routing of GIS surface meltwater Understanding the processes that govern surface meltwater routing on the Greenland Ice Sheet, and how this meltwater routing might change with changing climate or ice flow conditions, is important for understanding and predicting subglacial hydrology and ice sheet evolution. To examine processes that control ablation zone surface topography and meltwater routing, we have implemented analytical 2D transfer functions to predict the steady-state We implement linear transfer functions that predict the ice surface over rough bed topography and basal sliding variations, and applied them to multiple in multiple 2D regions of the western GIS ablation zone with near-uniform ice surface velocity.

We find Greenland Ice Sheet ablation zone. We verify that bed topography transfer alone can reasonably well explain at least, in the steady state limit, can largely explain ~ 1 -10 km wavelength ice surface topography, and show that given moulin locations bed topography also explains the observed routing patterns of surface meltwater. We thus infer that bed topography under a range of ice flow conditions, given sufficient quality bed DEMs.

We then apply flow-routing to extract supraglacial flow networks from observed ice surface DEMs and from bed topography transfer predicted ice surfaces. We quantify stream network conformity to surrounding topography and estimate the relation

between supraglacial channel slope and accumulated drainage area. These metrics are consistent with the inference that transfer of bed topography to the surface is the dominant process controlling general IDC-scale ($\sim 1-10$ km) surface-supraglacial meltwater routing on the GIS Greenland Ice Sheet ablation zone.

We demonstrate that bed topography transfer can be used. Finally, we conduct a parameter sensitivity study to predict the general response of surface topographic basins to changing adjustment of surface topography, supraglacial IDCs, and subglacial hydraulic potential that would occur in response to changing long-term averaged ice flow conditions in space or time. We propose a feedback by which the number density and size of IDCs are coupled to englacial input of meltwater that governs basal sliding efficacy, a representative western Greenland site. We show that the surface topography perturbations caused by changing ice flow can have direct effects on subglacial hydraulic pathways. However, the more significant impact on subglacial hydrology may result from the increasing number density of surface IDCs, and the corresponding dispersion of englacial/subglacial surface meltwater input, that we show would be caused by decreasing ice thickness or increasing long-term averaged basal sliding. This suggests a possible coupling between surface IDC configuration, subglacial hydrology, and basal sliding efficacy.

Code and data availability. All codes and data produced by the authors available upon request. Ice surface DEMs are from SETSM ArcticDEM 2-10 m resolution mosaics (ArcticDEM, 2017). Bed DEMs are from Icebridge BedMachine (Morlighem et al., 2014, 2015). Ice surface velocity data is from MEaSURES (Joughin et al., 2010b, a). 2015 Melt data is from RACMO 2.3p2 (Noel et al., 2015).

6

5.1 Time-Dependent Bed Topography and Basal Sliding Transfer Functions

We provide here a functional form of the ice surface transfer functions from Gudmundsson (2003) discussed in Section 2.3.1. We use the same notation as Gudmundsson (2003) except that we use k_U to denote wavenumber in the direction of ice velocity, and $*$ to denote non-dimensionalized variables.

All parameters are non-dimensionalized prior to solving (noted with $*$). Ice surface velocity U is non-dimensionalized by the zeroth-order deformational velocity $U^* = U \frac{2\eta}{\rho g H^2 \sin(\alpha)}$. Basal sliding coefficient C is non-dimensionalized as $C^* = C \frac{2\eta}{H}$. Thus the non-dimensional zeroth-order (mean) basal sliding coefficient C^{0*} represents the ratio of zeroth-order basal sliding velocity to zeroth-order surface deformational velocity, or the mean slip ratio. All spatial variables including absolute wave number k^* and wave number in the direction of ice flow k_U^* , are non-dimensionalized by scaling to H . Time is non-dimensionalized as $t^* = t \frac{\rho g H \sin(\alpha)}{2\eta}$.

The non-dimensionalized governing equations and boundary conditions are linearized around $\epsilon, \beta = 0$ and Fourier transformed (defined in Appendix ??). To obtain solutions the equations are Laplace transformed (as defined in Gudmundsson (2003)) in time. Solutions are in the form of transfer functions ($\hat{T}_B(k_x^*, k_y^*, t^*)$ and $\hat{T}_C(k_x^*, k_y^*, t^*)$) for the ice surface response to bed topography and basal sliding perturbations, defined at time t^* from perturbations at time $t^* = 0$ to B^{0*} or C^{0*} . These transfer

functions predict Z^* perturbations (where $Z^*(x^*, y^*, t) = Z^{1*}(x^*, y^*, t) + Z^{0*}(x^*, y^*)$) in response to basal topography or sliding perturbations ($B^{1*}(x^*, y^*, 0)$ or $C^{1*}(x^*, y^*, 0)$) as:-

$$\hat{Z}^{1*}(k_x^*, k_y^*, t^*) = \hat{T}_B(k_x^*, k_y^*, t^*) \hat{B}^{1*}(k_x^*, k_y^*, 0) + \hat{T}_C(k_x^*, k_y^*, t^*) \hat{C}^{1*}(k_x^*, k_y^*, 0)$$

Time-dependent bed topography transfer amplitude as a function of wave-number is-

$$5 \quad \hat{A}_B = \|\hat{T}_B\| = \frac{\tilde{a}}{\tilde{c} \sqrt{(\tilde{d}/\tilde{c})^2 + (\tilde{b}/\tilde{c})^2}} \sqrt{1 + e^{-t\tilde{b}/\tilde{c}} \left(e^{-t\tilde{b}/\tilde{c}} - 2 \cos(t\tilde{d}/\tilde{c}) \right)}$$

and bed topography transfer phase shift ϕ (in radians) is-

$$\hat{\phi}_B = \arctan \left(\frac{\mathbf{Im}(\hat{T}_B)}{\mathbf{Re}(\hat{T}_B)} \right) = \arctan \left(\frac{-\tilde{b} + e^{-t\tilde{b}/\tilde{c}} \left(\tilde{b} \cos(t\tilde{d}/\tilde{c}) - \tilde{d} \sin(t\tilde{d}/\tilde{c}) \right)}{\tilde{d} - e^{-t\tilde{b}/\tilde{c}} \left(\tilde{d} \cos(t\tilde{d}/\tilde{c}) + \tilde{b} \sin(t\tilde{d}/\tilde{c}) \right)} \right)$$

and basal sliding transfer amplitude is-

$$\hat{A}_C = \|\hat{T}_C\| = \frac{-\tilde{g}}{\tilde{c} \sqrt{(\tilde{d}/\tilde{c})^2 + (\tilde{b}/\tilde{c})^2}} \sqrt{1 + e^{-t\tilde{b}/\tilde{c}} \left(e^{-t\tilde{b}/\tilde{c}} - 2 \cos(t\tilde{d}/\tilde{c}) \right)}$$

10 and basal sliding transfer phase shift ϕ_C (in radians) is-

$$\hat{\phi}_C = \arctan \left(\frac{\mathbf{Im}(\hat{T}_C)}{\mathbf{Re}(\hat{T}_C)} \right) = \phi_B + \pi$$

where-

$$\tilde{a} = \left(U^* \tilde{f} + (U^* + k^{*2} C^{*(2)}) \cosh(k^*) \right) k^* k_U^*$$

$$\tilde{b} = (\tilde{f} \sinh(k^*) - k^*) \cot(\alpha)$$

$$15 \quad \tilde{c} = k^{*(3)} U^* + \tilde{f} k^* \cosh(k^*)$$

$$\tilde{d} = k_U^* U^* (\tilde{c} + k^*)$$

$$\tilde{g} = -k_U^* k^* C^* \cosh(k^*)$$

$$\tilde{f} = \cosh(k^*) + k^* C^* \sinh(k^*).$$

The ice surface perturbation propagation timescale (the time over which surface perturbations are advected down-flow by one wavelength) is given by:-

$$t_p^* = \tilde{c}/\tilde{b}$$

and the ice surface perturbation decay timescale (the timescale governing surface rise/depression rate from a basal perturbation) is given by:-

$$t_d^* = \tilde{c}/\tilde{d}.$$

5.1 Transfer Function Dependence on 2D Bed Topography

We use the bed topography transfer functions from Gudmundsson (2003) (and defined in Appendix ??) to demonstrate that predicted bed topography transfer amplitude and phase depend upon the angle θ of bed topographic features relative to the ice flow direction, as described in Section 2.3.2. By setting $k^* = k_U^* \cos(\theta)$ for a range of θ ($\theta \neq \frac{n\pi}{2}$), it can be shown that bed

5 topography transfer amplitude depends upon θ as

$$\hat{A}_B(\theta) = \left(k_U^{*(2)} \cos(\theta) \left(\cosh(k_U^* \cos(\theta)) \left(C^{0*(2)} k_U^{*(2)} \cos^2(\theta) + 2U^* \right) + C^{0*} k_U^* U^* \cos(\theta) \sinh(k_U^* \cos(\theta)) \right) \right) / \dots$$

$$\left(k_U^{*(4)} U^{*(2)} \cos^2(\theta) \left(\frac{1}{2} C^{0*} k_U^* \cos(\theta) \sinh(2k_U^* \cos(\theta)) + k_U^{*(2)} U^* \cos^2(\theta) + \cosh^2(k_U^* \cos(\theta)) + 1 \right)^2 + \dots \right.$$

$$\left. \cot^2(\alpha) \left(k_U^* \cos(\theta) (C^{0*} \sinh^2(k_U^* \cos(\theta)) - 1) + \frac{1}{2} \sinh(2k_U^* \cos(\theta)) \right)^2 \right)^{1/2}.$$

It can similarly be shown that bed topography transfer phase also depends upon θ as

$$\hat{\phi}_B(\theta) = -\operatorname{arccot} \left(\frac{k_U^{*(2)} v \tan(\alpha) \cos(\theta) \left(C^{0*} k_U^* \cos(\theta) \sinh(2k_U^* \cos(\theta)) + 2k_U^{*(2)} v \cos^2(\theta) + \cosh(2k_U^* \cos(\theta)) + 3 \right)}{2k_U^* \cos(\theta) (C^{0*} \sinh^2(k_U^* \cos(\theta)) - 1) + \sinh(2k_U^* \cos(\theta))} \right).$$

These equations give the potential variation in bed topography transfer amplitude and phase that could result from examining
 10 bed topography only along ice flowline transects, and thus demonstrate the importance of predicting the ice surface over 2D bed topography.

5.1 Fourier Transform

Fourier transforms are used in the derivation of the bed topography and basal sliding transfer functions. Via the convention of Gudmundsson (2003), the Fourier transform \mathcal{F} of a continuous function $f(x, y)$ is defined as

$$15 \quad \mathcal{F}(f(x, y)) = \hat{f}(k_x, k_y) = \int_{-\infty}^{\infty} \int_{-\infty}^{\infty} f(x, y) e^{i(k_x x + k_y y)} dx dy,$$

where k_x, k_y are wavenumbers in the x and y directions and $i = \sqrt{-1}$. The inverse Fourier transform is then

$$\mathcal{F}^{-1}(\hat{f}(k_x, k_y)) = f(x, y) = \frac{1}{4\pi^2} \int_{-\infty}^{\infty} \int_{-\infty}^{\infty} \hat{f}(k_x, k_y) e^{-i(k_x x + k_y y)} dk_x dk_y.$$

We use DFTs and inverse DFTs for both data processing and basal transfer function implementation, we calculate these on 1D and 2D data using Matlab version R2017b.

5.1 Conformity Metrics

We use two conformity metrics, %d and Λ , to examine how well stream network geometry is explained by surface topography lowpass filtered at various wavelengths as described in Section 2.4.4. We project stream networks onto filtered surfaces and then for each stream we calculate conformity factor as:-

$$5 \quad \Lambda = \frac{1}{L} \int_{l=1}^L \left| \frac{\mathbf{D}(l) \bullet (\nabla Z(l))}{\|\mathbf{D}(l)\| \|\nabla Z(l)\|} \right| dl$$

where $\|\cdot\|$ indicates vector magnitude, $\mathbf{D}(l) = (D_x(l), D_y(l))$ is the stream channel horizontal direction vector (the east-north direction of water flow, calculated with a 2nd order centered difference approximation of the stream channel tangent in map-view) at location l along a stream of length L , and $\nabla Z(l)$ is the corresponding ice surface gradient $\left(\frac{\partial Z}{\partial x} |_{l, \frac{\partial Z}{\partial y} |_{l}} \right)$ (calculated with a 2nd order centered difference approximation). We calculate percent downhill (here using discrete notation)

10 as:-

$$\%d = \frac{100}{N-1} \sum_{n=1}^{N-1} \begin{cases} 0 & \text{if } Z(n) \leq Z(n+1) \\ 1 & \text{if } Z(n) > Z(n+1) \end{cases}$$

where n indexes discrete location along a stream (n increases in the downstream direction), $Z(n)$ is the corresponding ice surface elevation, and N is the number of discrete locations along the stream, where each location corresponds to a DEM pixel. To calculate %d and Λ for a whole stream network we calculate %d and Λ for each stream segment in the network, then

15 take a weighted average of each metric over all stream segments, where data from each stream segment is weighted by the number of data points in that segment (N).

Author contributions. Josh Crozier implemented most modeling and data analysis with input from Leif Karlstrom and Kang Yang; the extraction of observed supraglacial stream networks was done by Kang Yang. Josh Crozier wrote the manuscript with input from Leif Karlstrom and Kang Yang. Leif Karlstrom, Kang Yang, and Josh Crozier conceived of the study.

20 *Competing interests.* No competing interests are present.

Acknowledgements. We thank Colin Meyer, Dan O'Hara, and Alan Rempel for their input and discussions. [We thank two anonymous reviewers for their constructive comments.](#) LK acknowledges funding from NASA award NNX16AQ56G. [Kang Yang acknowledges support from the National Natural Science Foundation of China \(41501452\) and the Fundamental Research Funds for the Central Universities.](#)

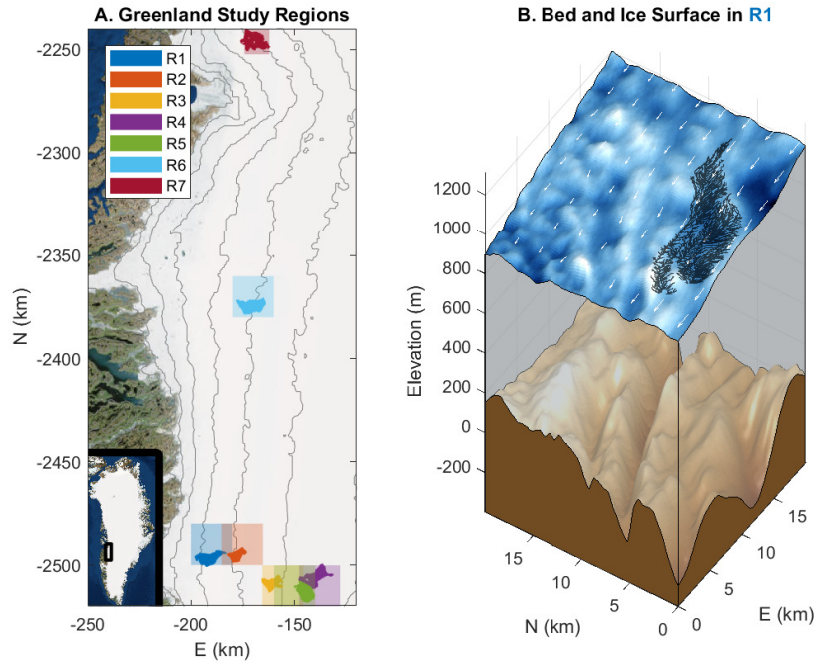


Figure 1. (A) Study ~~IDs~~ IDs (solid colored patches) ~~on the of~~ of western ~~GIS~~ GIS Greenland with bounding boxes (semi-transparent squares) indicating corresponding domain used for bed transfer and admittance calculations. Black 200 m elevation contours are from BedMachine/GIMP (Howat et al., 2014; Morlighem et al., 2017a). Imagery is from ArcGIS ERSI world imagery basemap. ~~500-m elevation contours (black) and ice surface velocity field (white arrows) are from sources cited in (Section 2.1).~~ 500-m elevation contours (black) and ice surface velocity field (white arrows) are from sources cited in (Section 2.1). The black star in SE Greenland (submap) indicates the ~~location of an additional region RSF we study that does not exhibit supraglacial streams.~~ location of an additional region RSF we study that does not exhibit supraglacial streams. Information on all regions is shown in Table ?? . (B) Ice surface and bed ~~elevation elevations~~ elevation elevations (from BedMachine/GIMP) in study region R1, with stream channels from study drainage network shown in black and velocity field shown by white arrows.

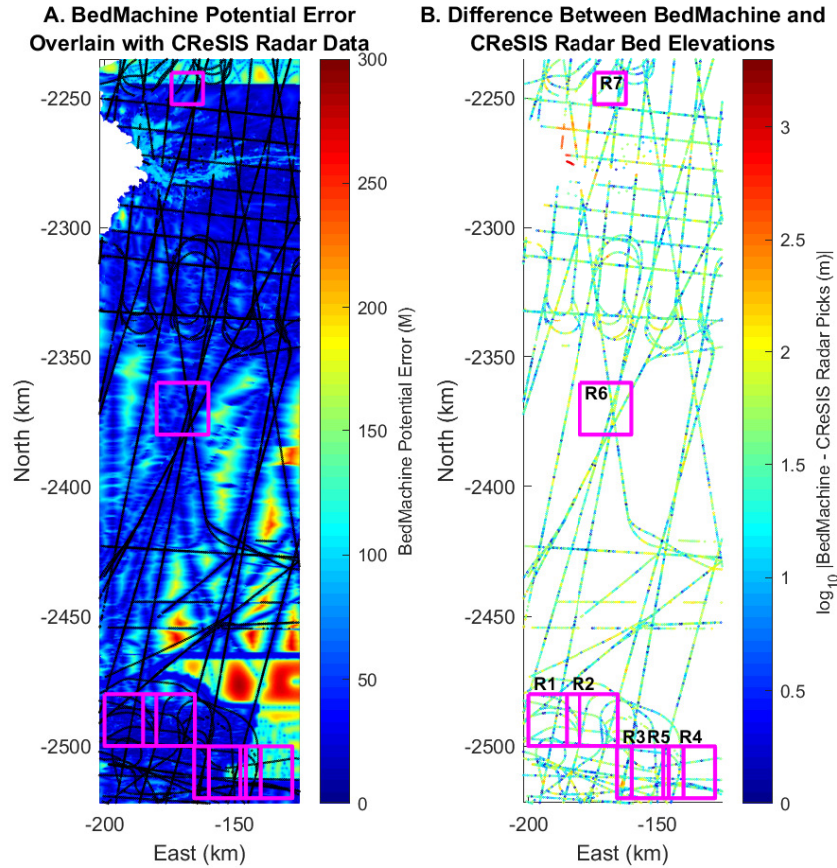


Figure 2. (A, B) 2D-BedMachine v3 potential bed topography transfer function amplitude and phase, as defined in Appendix ?? elevation error overlay by CReSIS radar bed elevation picks (Morlighem et al., 2017a, b; CReSIS, 2016). White arrows in both plots indicate ice flow direction. Ice flow parameters used are BedMachine includes radar data from other sources not shown here, and is also constrained with mass conservation modeling over most of the region R1 shown. BedMachine error generally decreases where elevations are better constrained by radar data. Our study regions (magenta) encompass a broad range of bed DEM quality (Fig. 1.A, Table ??) with $\eta = 10^{14}$ Pa s. (B) Difference between bed elevations from BedMachine and $C^{0*} = 11$ CReSIS radar picks (only including radar picks marked as good quality). In many regions there is appreciable scatter in radar elevation picks and significant error in the derived bed DEM; we examine the impact this uncertainty has on ice surface predictions.

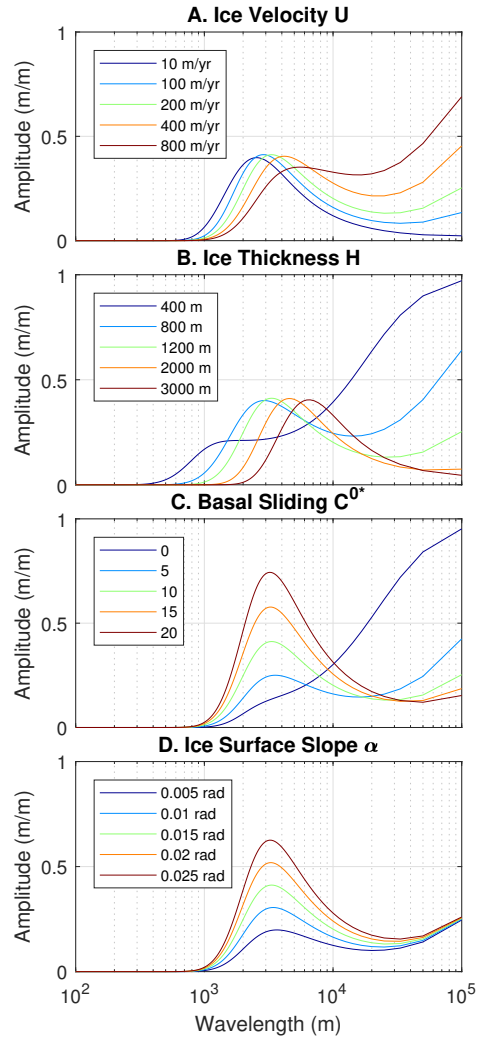


Figure 3. (A-D) Bed topography transfer function amplitudes in the ice flow direction (along an ice flowline). In all plots the parameters not otherwise indicated are: $U = 100$ – $U = 200$ m/yr, $H = 1000$ – $H = 1200$ m, $C^{0*} = 10$, $\alpha = 0.01$ – $\alpha = 0.015$ radians, and $\eta = 10^{14}$ Pa s. The spread of plotted parameters broadly encompasses the range of parameters found in our study regions (Fig. 1.A, Table ??). Transfer amplitude peaks between around 1-10 km for a wide range of parameters.

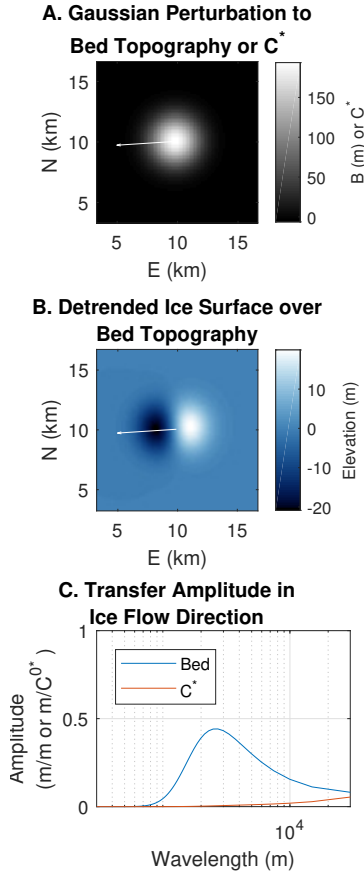


Figure 4. Effect-illustration of 2D bed topography on ice flowline bed topography steady state basal transfer amplitude, defined in Appendix ??. $A(\theta)$ is predicted transfer amplitude for ice flowline equivalent bed topography aligned at angle θ from the ice flow direction, and $A(0)$ is parameters representative of the predicted flowline-only (equivalent to $\theta = 0$) transfer amplitude western Greenland ablation zone. Ice flow parameters used are from region R1 (Fig. 1.A, Table ??) with $\eta = 10^{14}$ Pa s. (A) Gaussian bed topography or basal sliding perturbation. (B) Detrended predicted ice surface over the Gaussian bed topography perturbation (with $C^{0*} = 10$). White arrows in plots A and $C^{0*} = 11$ B indicate the ice flow direction. (C) Transfer amplitudes in the ice flow direction (along a flowline) for bed topography and basal sliding C^* perturbations. The transfer functions also have important phase components not shown here (see Gudmundsson (2003)). With these flow parameters, surface topography created from basal sliding perturbations should generally be of much lower amplitude than surface topography created from bed topography.

(A) Gaussian bed topography or basal sliding distribution. (B, C) Detrended predicted ice surface over basal perturbations. White arrows in (A, B, C) indicate ice flow direction. (D) The discrete Gaussian amplitude spectrum appears different from a continuous Gaussian amplitude spectra. (E, F) Transfer amplitudes and phases in ice flow direction. All ice flow parameters (other than bed topography and basal sliding) are from region R1 (Fig. 1.A, Table ??) with $\eta = 10^{14}$ Pa s and $C^{0*} = 11$ for the Gaussian bed topography test case (B).

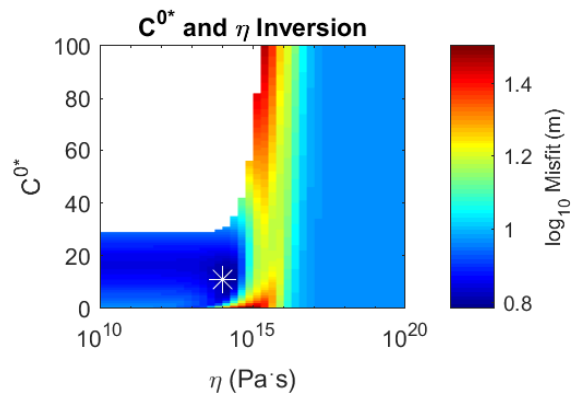


Figure 5. Misfit minimization for η and C^{0*} between the ice surface DEM and bed topography transfer predicted ice surfaces in study region R1 (Fig. 1.A, Table ??). White star indicates the location of minimum misfit, at $C^{0*} = 10$ and $\eta = 10^{14}$. Blank plot area is the region where parameters are nonphysical (resulting in transfer amplitudes > 1).

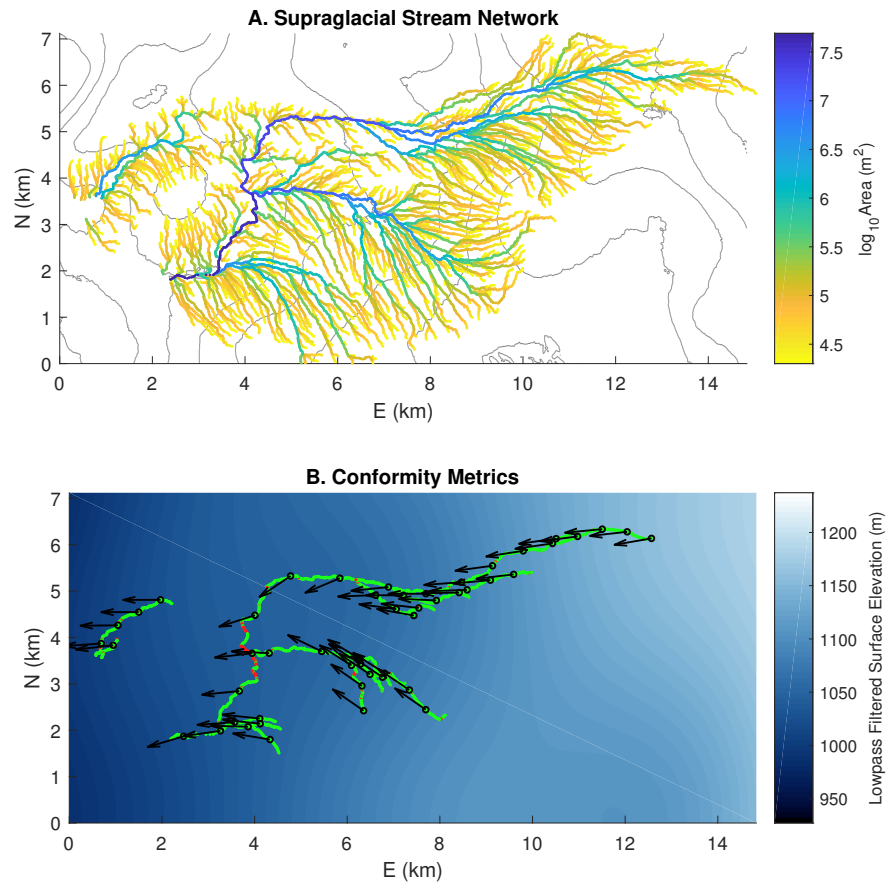


Figure 6. (A) Bed-DEM-Supraglacial stream network obtained by flow-routing on 2 m DEMs from study region R1 (Fig. 1.A, Table ??), colored by accumulated upstream drainage area. Surface elevation is shown with 20 m black contours. Fluvial incision rate should increase with increasing slope and drainage area (Eq. 7). (B) Bed-DEM-error Illustration of stream conformity metrics for select streams from the same network, projected onto topography lowpass filtered at a 6 km cutoff wavelength. White boxes in Sections of streams that would be flowing uphill on this filtered surface are colored red and other sections are green; this data is used to calculate percent downhill %d. Black arrows indicate steepest descent directions on this filtered surface; the angle between these directions and the corresponding stream channel orientations is used to calculate conformity factor Λ .

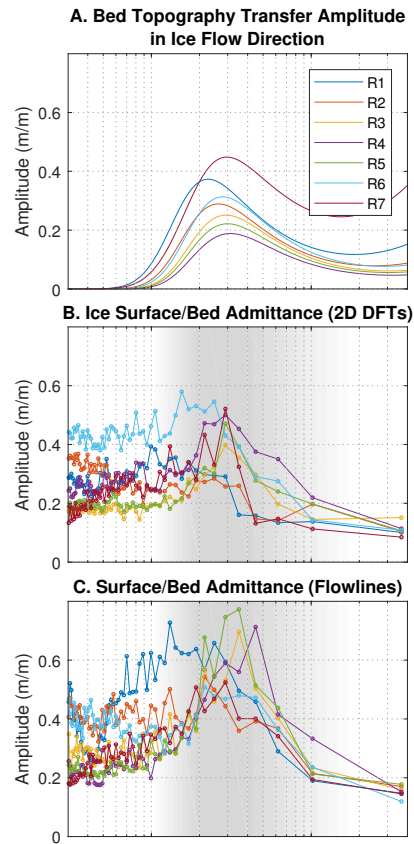


Figure 7. (A) Predicted bed topography transfer amplitudes from our seven study regions (Fig. 1.A, Table ??), with $\eta = 10^{14}$ Pa s and $C^{0*} = 10$ in all regions. (B, C) indicate the region—Two different calculations of the empirical bed over which the topography admittance to ice surface is topography (Section 2.3.5). For all regions, both calculations of admittance generally match predicted transfer amplitudes at wavelengths greater than ~ 1 km, and exhibit similar amplitude peaks.

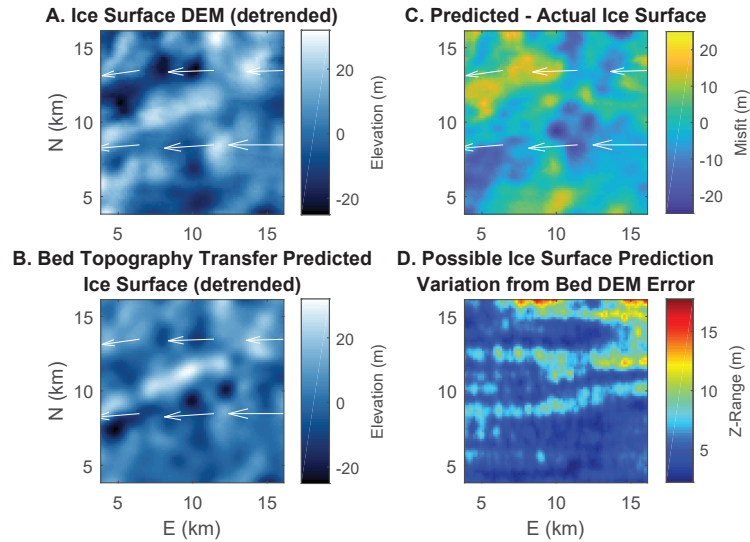


Figure 8. [Example ice surface prediction and error analysis from study region R1 \(Fig. 1.A, Table ??\)](#). (A) Detrended ice surface DEM. (B) Detrended bed topography transfer predicted ice surface, with $\eta = 10^{14}$ Pa s and $C^{0*} = 11$, $C^{0*} = 10$. We note that km-scale depressions and ridges/peaks are generally configured similarly to the real ice surface DEM in plot A, and that topographic relief also corresponds well. (C) Prediction misfit (subtraction between the actual (A) and predicted (B) ice surfaces in plots A and B). Though the prediction misfit is often large/significant, $\sim 1-10$ m which might be expected for a number of reasons discussed in Sections [km-scale topographic features are well predicted](#) 2.1, 2.3.1, and 2.3.2. (D) Potential effects of bed DEM error on ice surface predictions (see error map in Fig. 2.A). Where bed DEM error is less than ~ 60 m the potential surface prediction variation is much less than the amplitude of surface topography. White arrows in all plots indicate ice surface velocity field, and the bed DEM underlying this region is shown in Fig. 1.B.

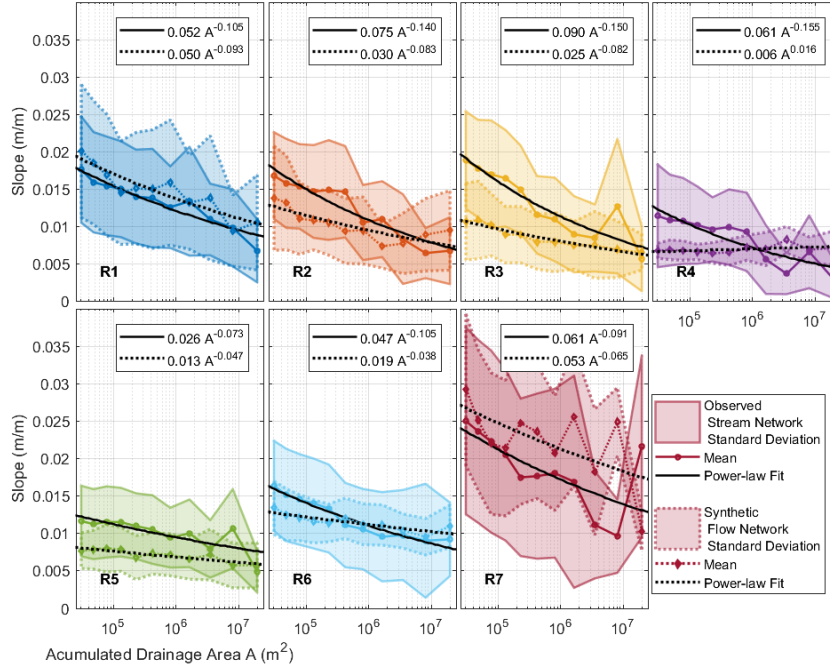


Figure 9. (A) Stream-Mean stream channel slope-slopes binned by accumulated upstream drainage/flow area from supraglacial-stream networks-in-our seven study regions (Fig. 1.A, Table ??). (B) Synthetic-flow-networks-Results are shown from a stream-free area of the GIS (FN-RSF) both observed supraglacial stream networks and from two synthetic flow networks calculated on bed topography transfer predicted ice-surfaces (FN-BTT-R1 see Sections 2.4.2 and FN-BTT-R2 2.4.3). The standard deviation of slope within each area bin is indicated by shaded patches, where patches with the corresponding supraglacial solid outlines correspond to observed stream networks and patches with dotted outlines to synthetic flow networks. Mean slopes are shown for comparison (by solid blue and orange dotted colored lines and power law fits by solid and dotted black lines. Synthetic flow networks from regions R3, identical R4, R5, and R6 may not be meaningful due to the curves in surface under-prediction (A see Section 3.2)).

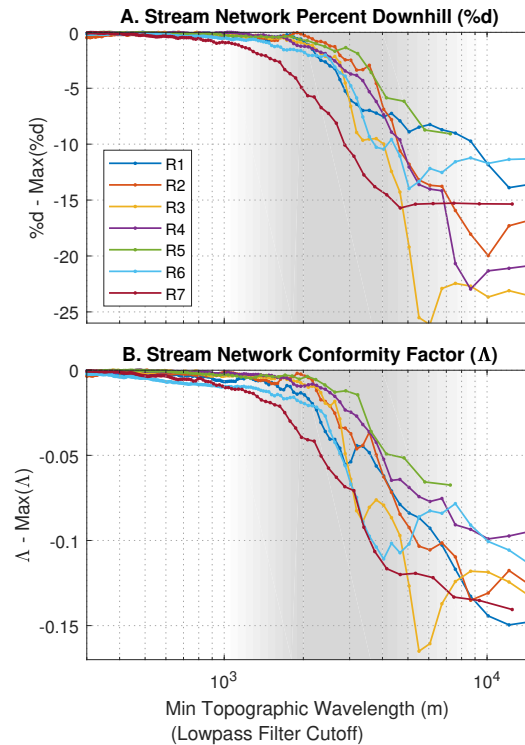


Figure 10. (A) Percent downhill $%d$. (B) Conformity factor Λ . Values for both stream metric topographic conformity metrics are calculated in our seven study regions, ~~plus synthetic flow networks from the stream-free study region FN-RSF and from two bed topography transfer predicted ice surfaces FN-BTT-R1 and FN-BTT-R2~~ (Fig. 1.A, Table ??). All values are normalized to the maximum values in each network due to the variability in plateau values of $%d$ and Λ between networks. For all supraglacial stream networks ~~and synthetic flow networks~~ the only cutoff filter wavelengths over which $%d$ and Λ change significantly are between ~ 1 -10 km, similar to the bed topography wavelengths predicted to transfer most strongly.

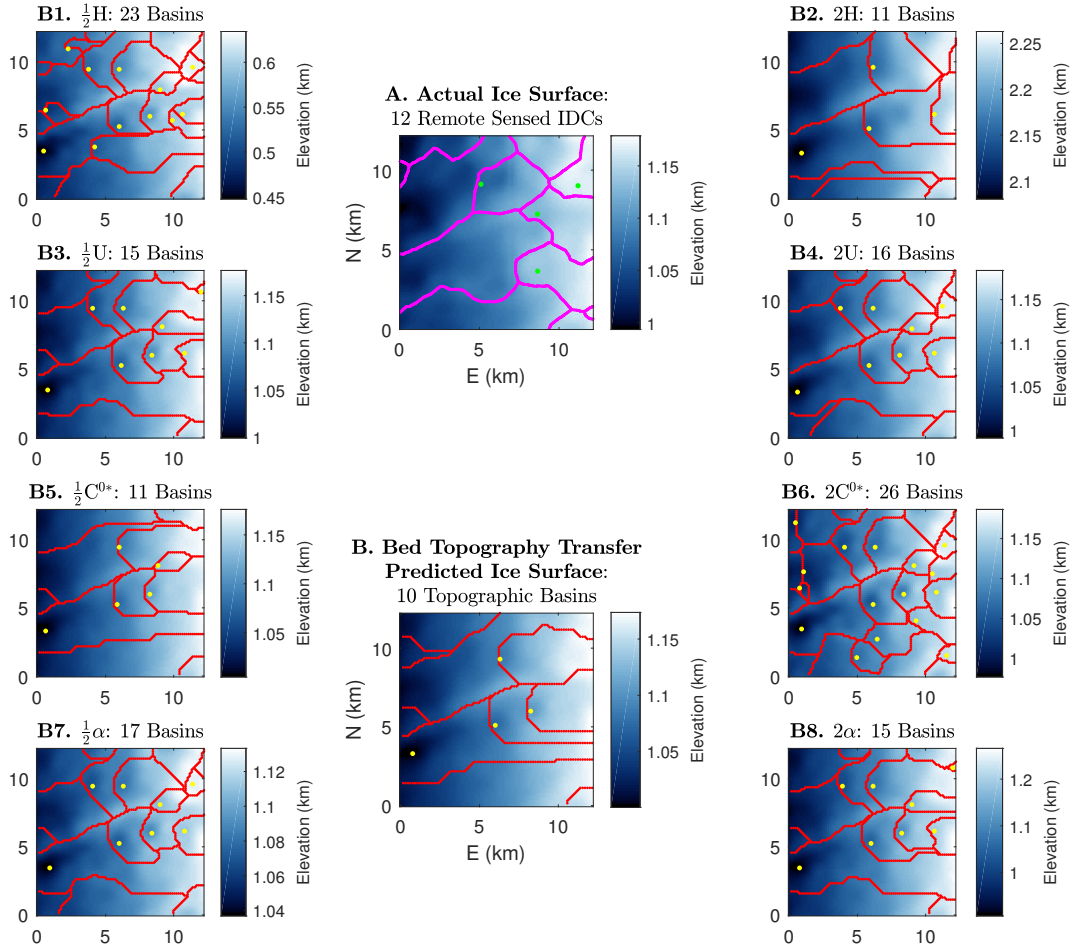


Figure 11. (A) IDCs (magenta outlines) and moulin (green dots) obtained from satellite images by (Yang and Smith, 2016). (B, B1-B8) Ice Surface topographic basins (red outlines) and local minima (yellow dots) on bed topography transfer predicted ice surfaces with various ice flow parameters. From study region R1 (Fig. 1.A, Table ??) with $\eta = 10^{14}$ Pa s and $C^{0*} = 11$ baseline $C^{0*} = 10$. While the bed transfer predicted topographic basin configuration (in plot B) is different from the IDC configuration (in plot A), the basin densities are similar. Changing ice thickness H or basal sliding parameter C^{0*} by factors of two produces significant changes in predicted topographic basin configurations (B1-B2 and B5-B6).

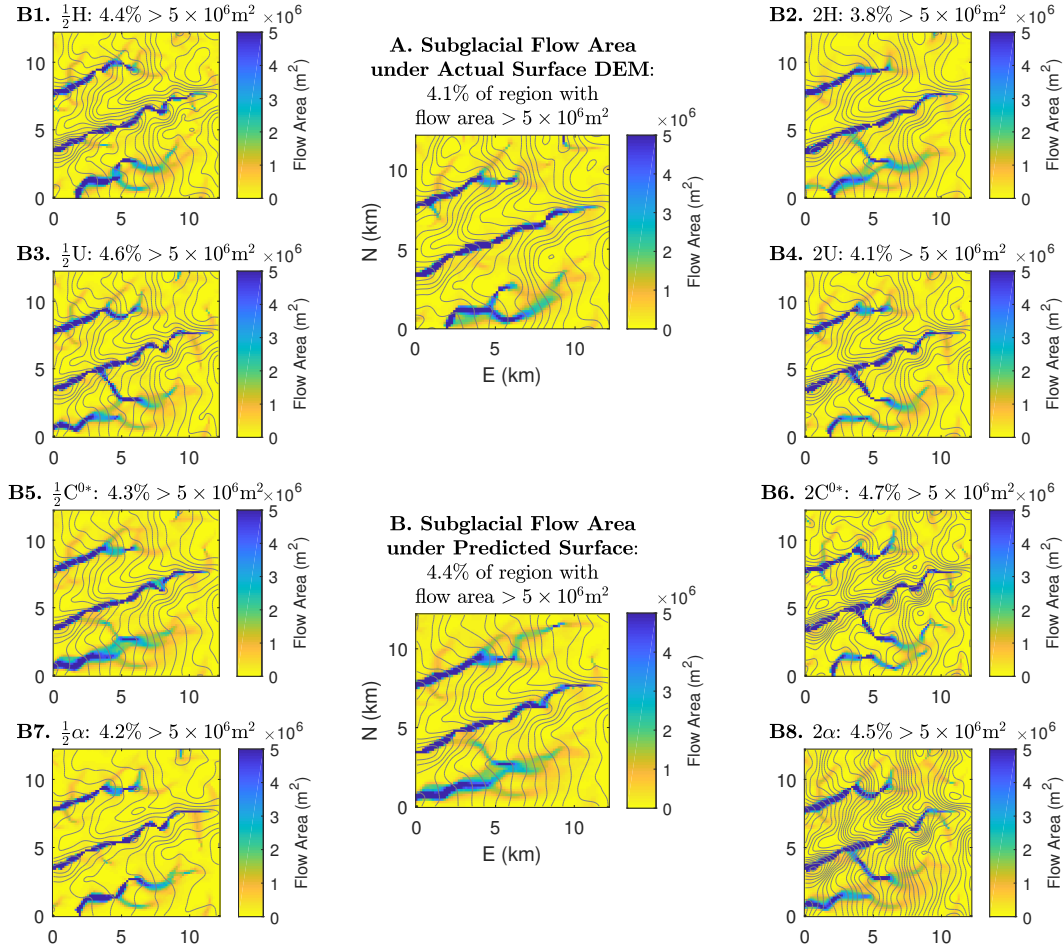


Figure 12. (A) Subglacial accumulated flow (drainage) area obtained via flow-routing on hydraulic potential fields calculated under the actual ice surface DEM from BedMachine/GIMP, (Howat et al., 2014; Morlighem et al., 2017a). Grey contours in all plots are 0.1 MPa hydraulic potential contours. (B, B1-B8) Subglacial accumulated flow area calculated under the bed topography transfer predicted ice surface with various ice flow parameters. From study region R1 (Fig. 1.A, Table ??) with $\eta = 10^{14} \text{Pa s}$ and baseline $C^{0*} = 10$. The flow-area threshold displayed ($5 \times 10^6 \text{m}^2$) was chosen to highlight pathways of high relative water flux.